Renormalization of thermal fluctuations by heterogeneous damage for macroscopic rupture processes

Didier Sornette
Chair of Entrepreneurial Risks, ETH-Zurich
(Swiss Federal Institute of Technology, Zurich)
Department of Management, Technology and Economics
http://www.er.ethz.ch/

with A. Saichev (Nizhny-Novgorov) and G. Ouillon (Nice)

Experiments by Zhurkov Int. J. Fract. Mech. **1**, 311 (1965)

$$\text{Ln}\,\tau = A - B\,\sigma$$

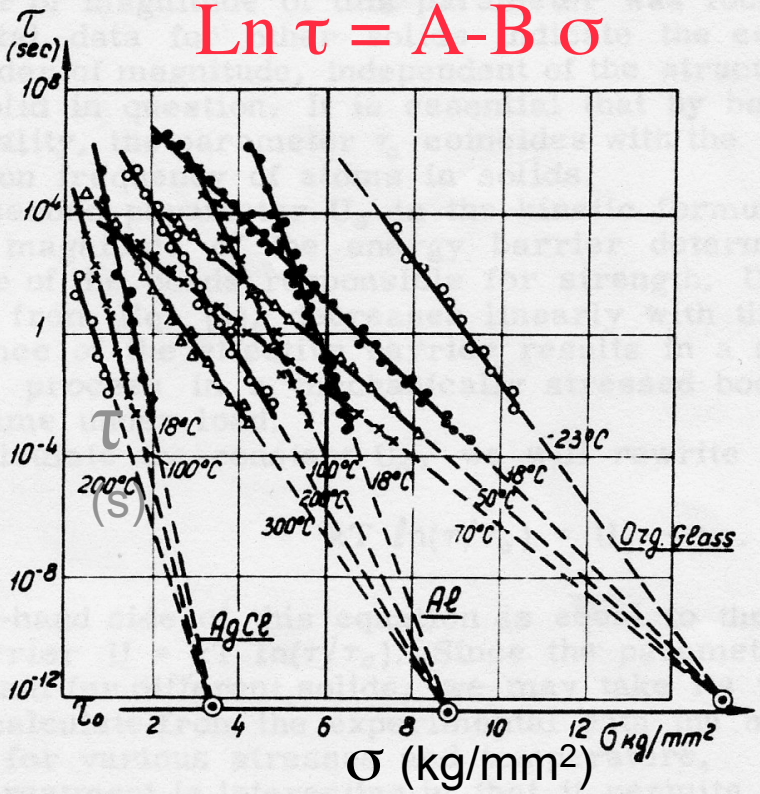

Fig. 5. Time and temperature dependence of the lifetime of solids on stress.
1. Silver chloride (Reference 4)
2. Aluminum (Reference 5)
3. Plexiglas (Reference 6)

$$\tau = \tau_0 \exp\left(\frac{U}{k_B T}\right)$$

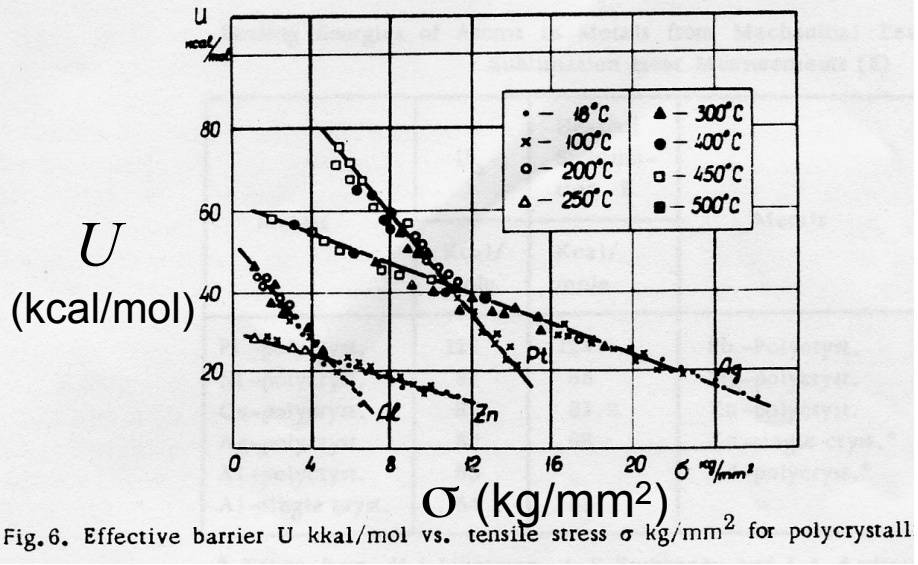

Fig. 6. Effective barrier U kkal/mol vs. tensile stress σ kg/mm^2 for polycrystall

Empirical energy barrier

$$U = U_o - \alpha\sigma$$

où U_o : énergie de sublimation

A possible mechanism : thermal activated process

Penny-shaped crack

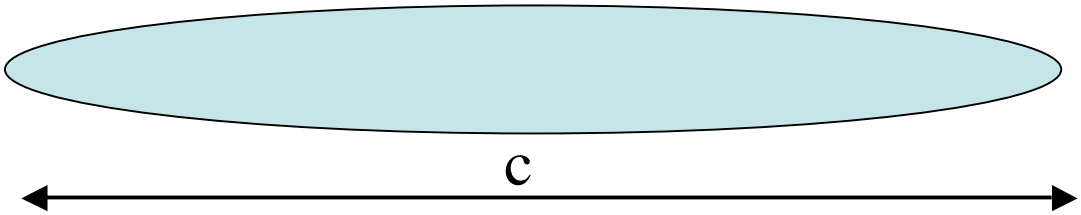

$$\text{Griffith energy} \approx g\ c^2 \quad = kT_d$$

$g = 10 - 50$ erg/cm^2 for most solids.

Importance of thermal fluctuations: $\mu = \sqrt{T_d/T}.$

$$\mu \approx 1.5 - 4 \cdot 10^3 \quad c = 1 \text{ micron}$$

$$\mu \approx 1.5 - 4 \text{ for } c = 1 \text{ nanometer}$$

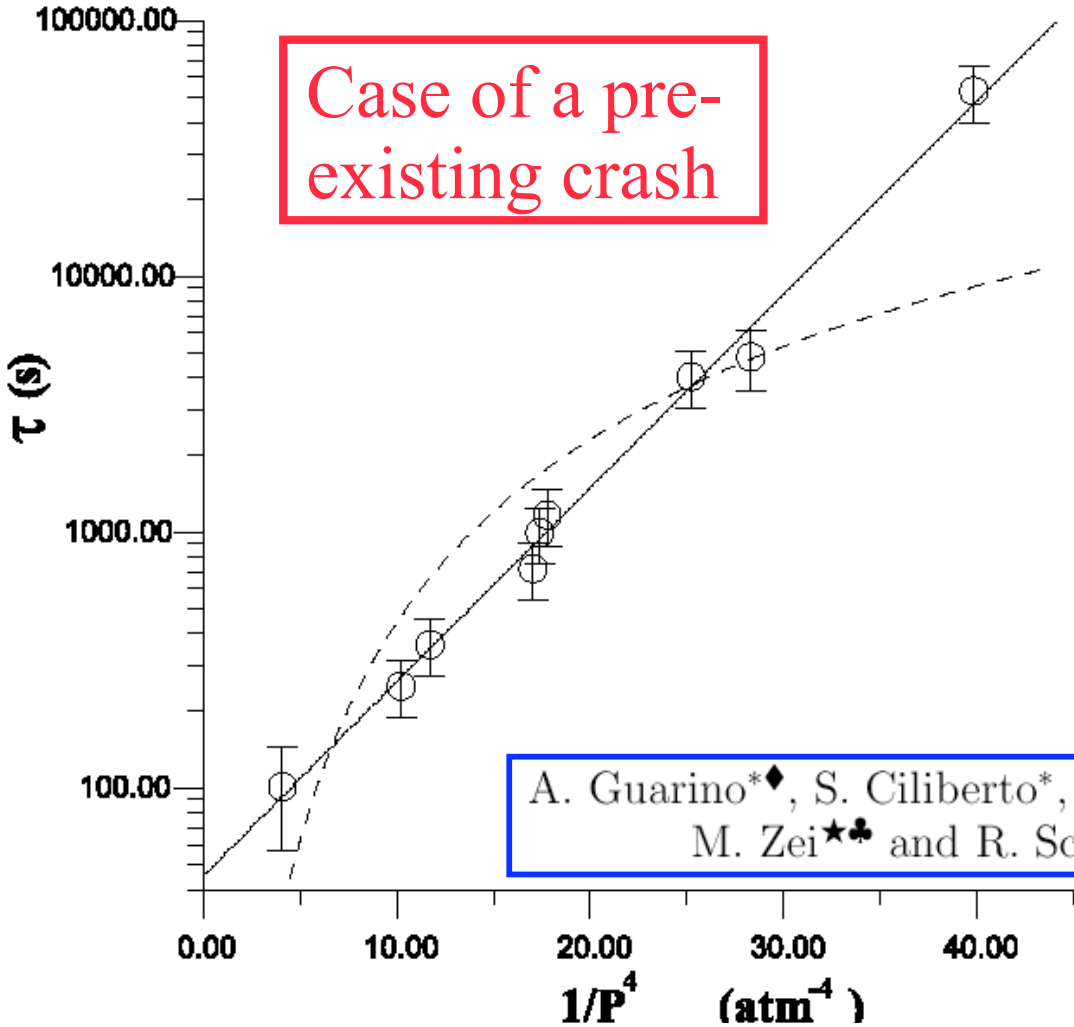

Case of a pre-existing crash

$$\tau = \tau_o \exp\left(\frac{P_o}{P}\right)^4$$

$$P_o = G\left(\frac{\eta^3 Y^2}{KT}\right)^{1/4}$$

η: surface energy

Y: elastic modulus

A. Guarino*♦, S. Ciliberto*, A. Garcimartín‡, M. Zei★♣ and R. Scorretti*♡ (2002)

Figure 4: Measurements on wood samples. The time τ needed to break the wood samples under an imposed constant pressure P is here plotted as a function of $1/P^4$ in a semilog scale. The dashed line represents the solution proposed by Mogi [20]($\tau = ae^{-bP}$). The continuous line is the solution proposed by Pomeau for microcrystals ($\tau = \tau_o e^{(P_o/P)^4}$). In the plot $\tau_o = 50.5$ s and $P_o = 0.63$ atm. Every point is the average of 10 samples. The error bar is the statistical uncertainty. For the fiberglass samples, we find $\tau_o = 44.6$ s and $P_o = 2.91$ atm.

A theory of deformation processes needs two ingredients:

1. the identification of the relevant microscopic objects controlling the deformation. These defects can be dislocations, grain boundaries, micro-cracks, vacancies and micro-voids;

2. the interplay and cooperative behavior of all these defects which lead to the deformation.

$$E(R) = a\alpha R^2 - b\frac{\sigma^2 R^3}{Y}$$

$$R_c = \frac{2a\alpha Y}{3b}\frac{1}{\sigma^2} \qquad E^* \sim \frac{1}{\sigma^4}$$

$$rate \sim e^{-\frac{E^*}{k_B T}}$$

Selinger et al (1991)
Golubovic and Feng (1991)
Pomeau (1992)

Failure time and critical behaviour of fracture precursors in heterogeneous materials

A. Guarino*♠, S. Ciliberto*, A. Garcimartín‡,
M. Zei★♣ and R. Scorretti*♡

In fact we changed temperature, from $300K$ to $380K$ which is a temperature range where the other parameters, Y and η, do not change too much. For this temperature jump one would expect a change in τ of of about 50% for the smallest pressure and of about 100% for the largest pressure. Looking at fig. 8 we do not notice any change of τ within experimental errors which are about 10%. In order to maintain the change of τ within 10% for a temperature jump of $80K$ one has to assume that the effective temperature of the system is about $3000K$. Notice that this claim is independent on the exact value of the other parameters and G.

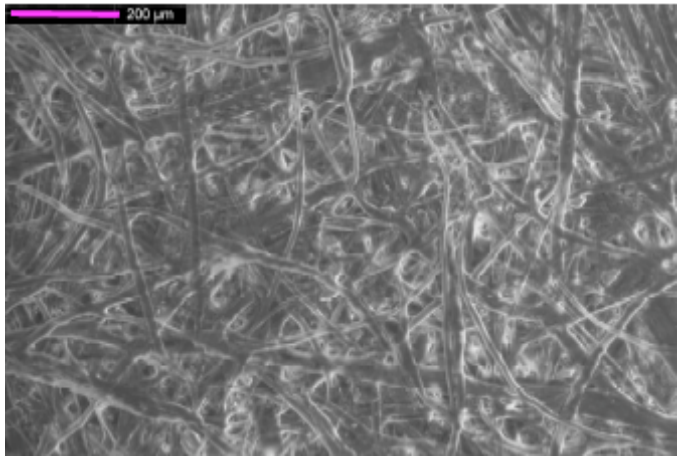

Paper sheets

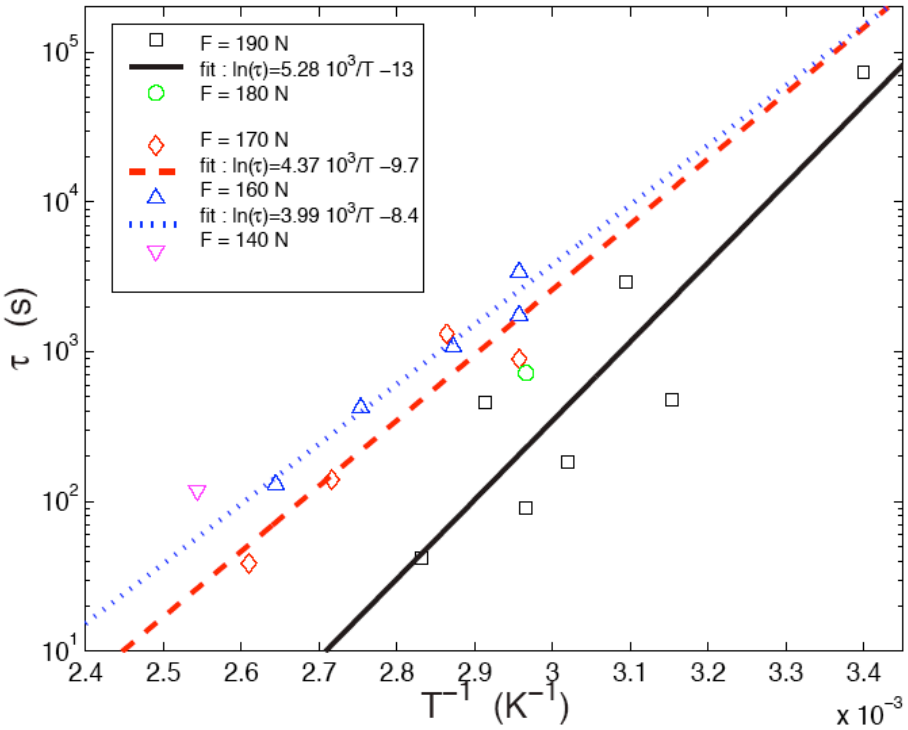

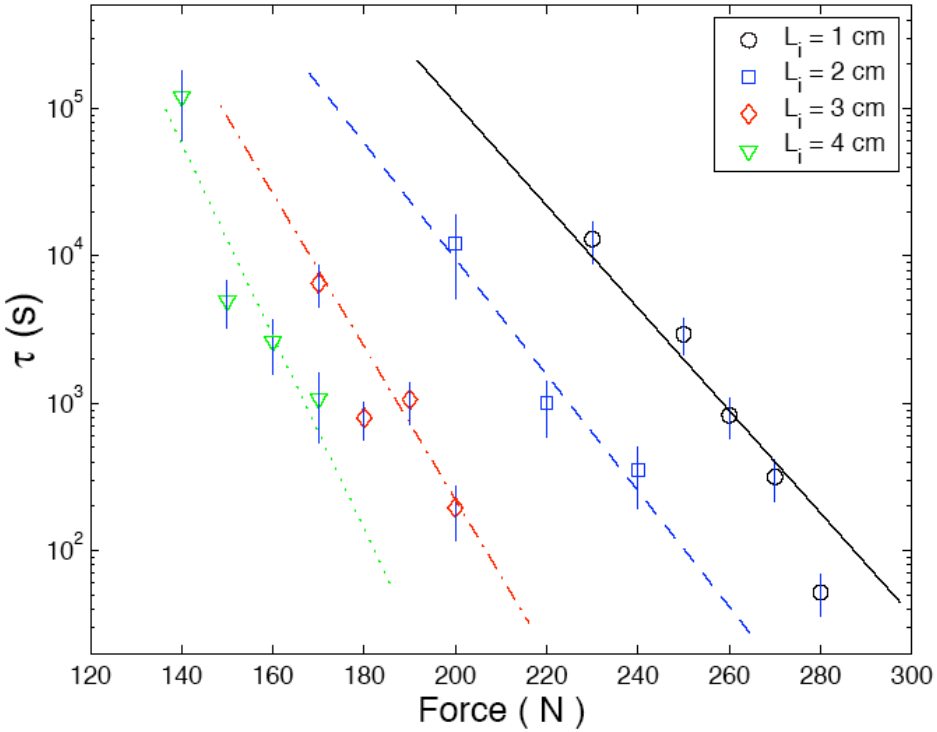

Stéphane Santucci, Loïc Vanel, Sergio Ciliberto (2004)

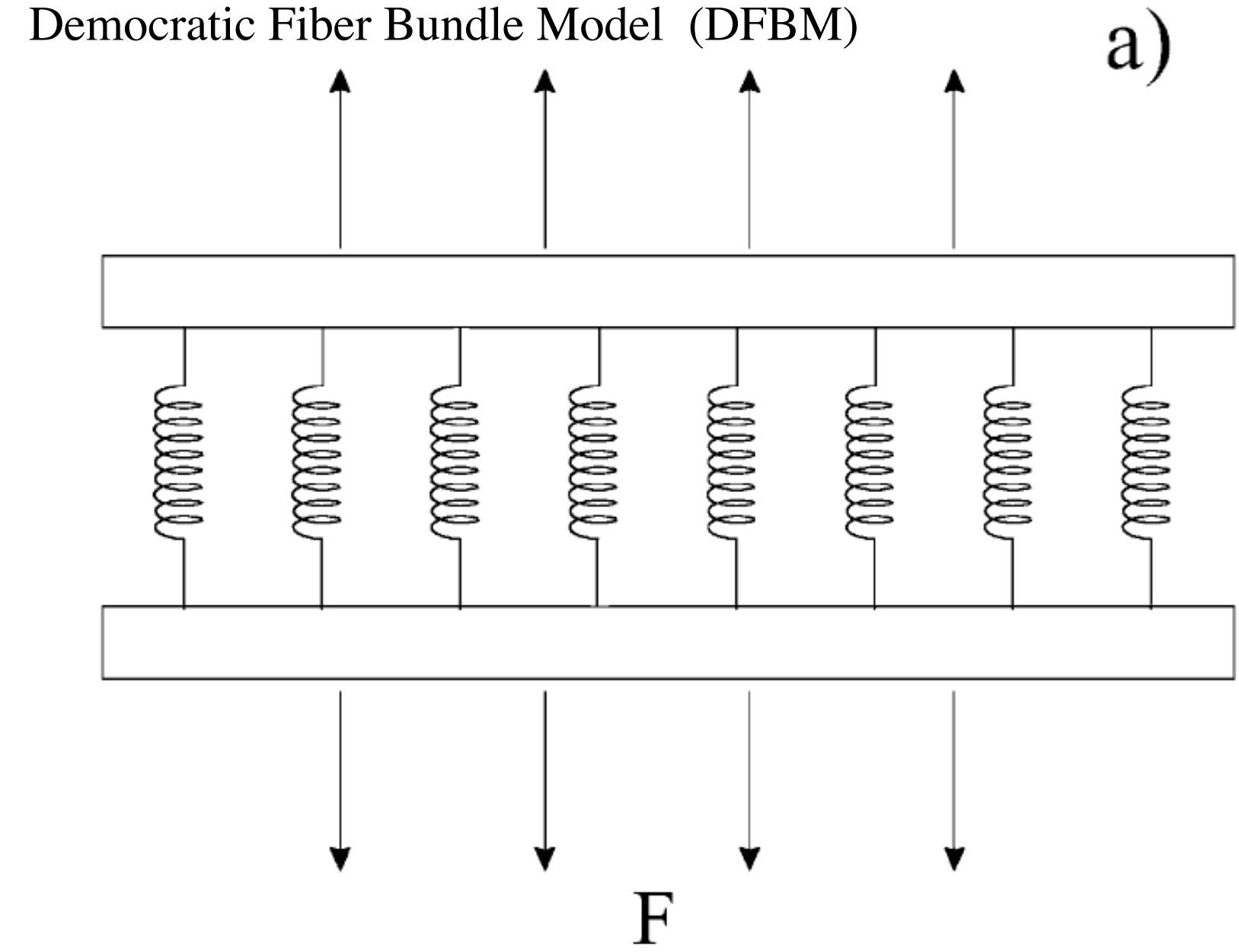

1. S. Roux and F. Hild, On the relevance to meanfield in continuous damage mechanics, Int. J. Fract. 116, 219 (2002)
2. F. Reurings and M. J. Alava, Damage Growth in Random Fuse Networks (http://arXiv.org/abs/cond-mat/0401592)

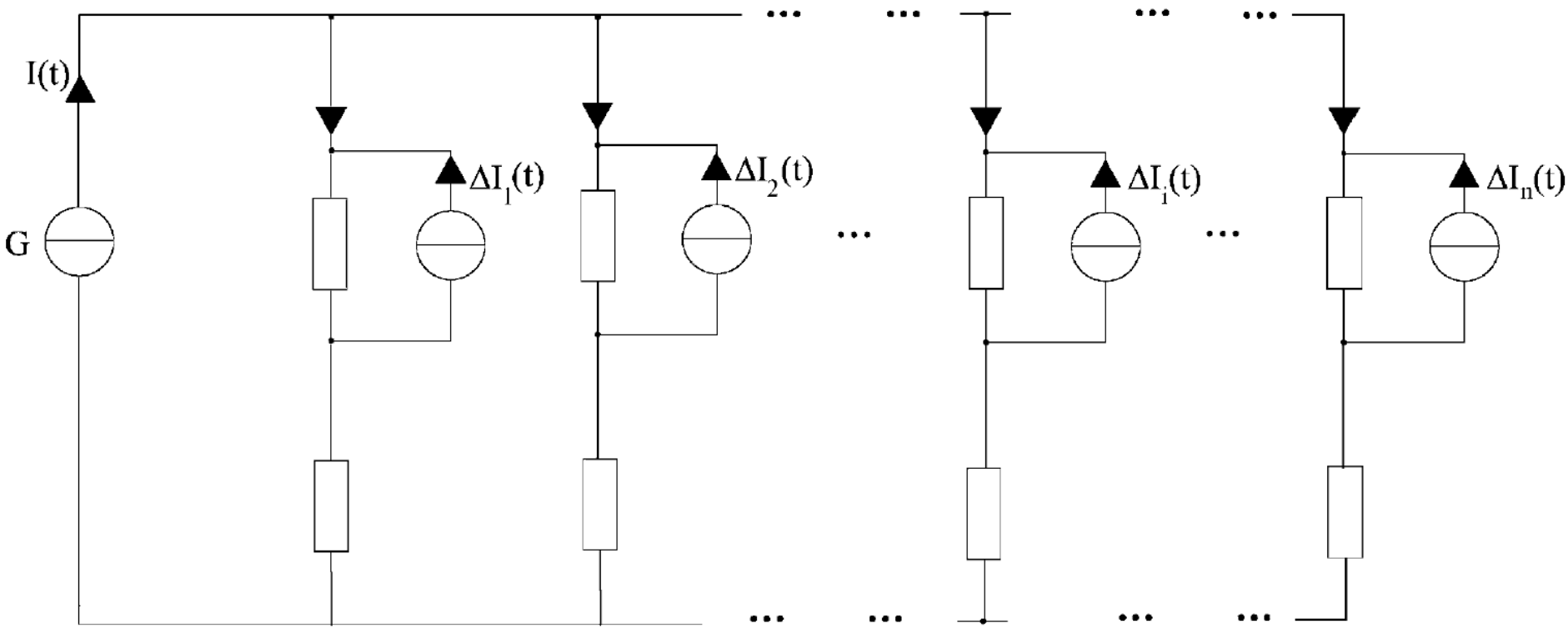

$$f_i(t) = \frac{f_0 N}{N - n(t)} + \Delta f_i(t)$$

Fig. 1. (a) Modified DFBM: N fiber in parallel, with the edges fixed on a rigid support are subjected to an externally imposed force F which is distributed democratically on the net, i.e., all fibers (not broken) are affected in the same way. Each fiber is also subjected to a random (zero mean, normally distributed), addictive force $\Delta f_i(t)$, where it is intended that $\Delta f_i(t)$ is a realization of a white, time-independent stochastic process. Name $n(t)$ the number of broken fibers at time t; we derive the following expression of local force f_i for the ith fiber: $f_i = (F/(N-n(t))) + \Delta f_i$. (b) The equivalent of the fiber bundle model is the fuse network. One can think to our model as a fuse network where the Nyquist noise of several resistances (current generators ΔI_i) are the noise generators for each bond.

$$f_i(t) = \frac{f_0 N}{N - n(t)} + \Delta f_i(t)$$

thermal fluctuations

Condition for rupture:

non-zero probability $G(f_c(i) - f_a)$ for $\Delta f_i \geq f_c(i) - f_a$

$$G(f_c(i) - f_a) = \frac{\gamma}{2} \operatorname{erfc}\left(\frac{f_c(i) - f_a}{\sqrt{2T}}\right)$$

is the rate for the fiber i to fail under the force f_a
given its rupture threshold $f_c(i)$

Quenched disorder $P_d(f) = \frac{1}{\sqrt{2\pi T_d}} \exp\left[-\frac{(1-f)^2}{2T_d}\right]$

fraction of broken fibers at time t

$$\text{by definition } \Phi(t) = 1 - \int_{-\infty}^{+\infty} df \; Q(f,t)$$

Force "rupture front" approximation:

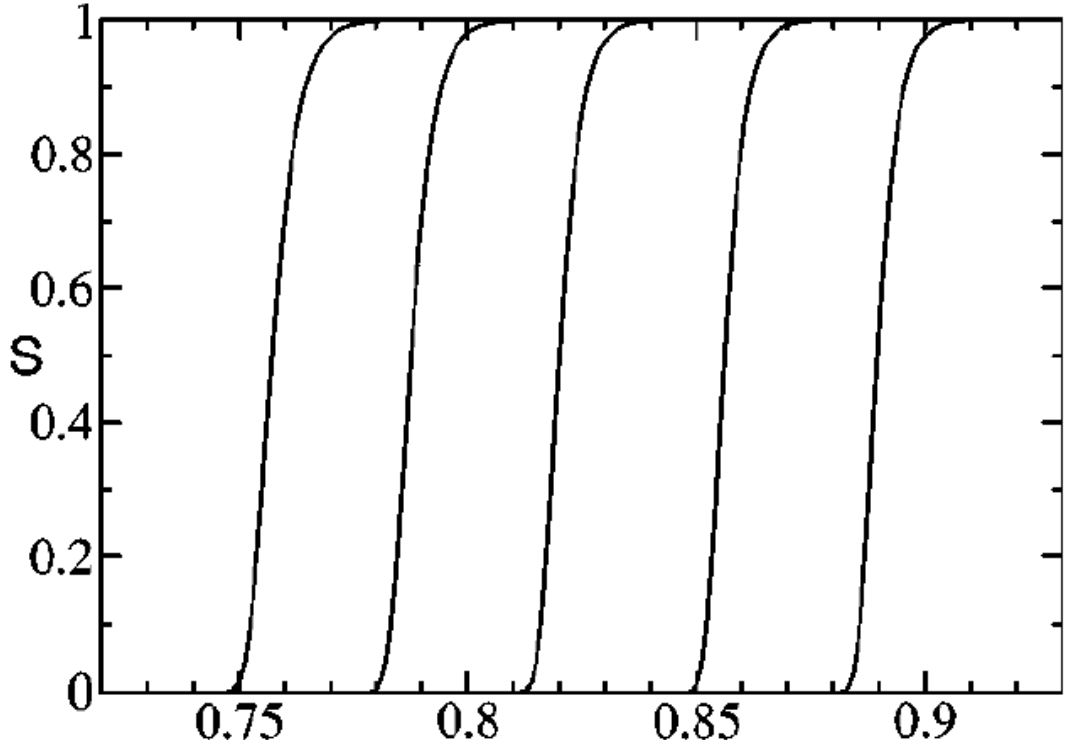

POLITI, CILIBERTO, AND SCORRETTI
PHYSICAL REVIEW E **66**, 026107 (2002)

$S(t) = Q(f,t)/P_d(f)$

pdf of unbroken fibers

$$Q(f,t) = P_d(f) \;, \quad \text{for } f > f_s(t)$$

excellent approximation

$$\Phi(t) = \int_{-\infty}^{f_s(t)} df \; P_d(f)$$

$$\Phi(t) = 1 - \int_{-\infty}^{+\infty} df\, Q(f,t)$$

$$dQ(f,t)/dt = -Q(f,t)\, G(f - f_a)$$

$$\dot{\Phi} = \frac{\gamma}{2} \int_{f_s}^{\infty} \frac{1}{\sqrt{2\pi T_d}} \exp\left[-\frac{(1-f)^2}{2T_d}\right] \operatorname{erfc}\left(\frac{f - f_a}{\sqrt{2T}}\right) df$$

$$\Phi(t) = \int_{-\infty}^{f_s(t)} df \; P_d(f)$$

$$\Phi = \frac{1}{2}\left[\mathrm{erf}\left(\frac{f_s - 1}{\sqrt{2T_d}}\right) + 1\right], \; f_s = 1 + \sqrt{2T_d}\,\mathrm{irf}\,(2\Phi - 1)$$

irf: inverse to error function

$$\dot{\Phi} = R(\phi) \equiv \frac{\gamma}{2}\int_{\Phi}^{1} \mathrm{erfc}\,[L(\Phi, z)]\, dz\,,$$

$$L(\Phi, z) = \frac{1}{\sqrt{2T}}\left(1 - \frac{f_0}{1 - \Phi}\right) + \mu\,\mathrm{irf}\,(2z - 1)$$

$$\mu = \sqrt{T_d/T}$$

For μ>1, linearize L which gives

$$\dot{\Phi} = R(\Phi) = \frac{\gamma T}{4\pi\mu D(\Phi)U(\Phi)}\, e^{-U(\Phi)/T},$$

where

Energy barrier between the applied force per fiber and the "front force"

$$U(\Phi) = TL^2(\Phi,\Phi) = \frac{1}{2}\left[f_s(\Phi) - f_a(\Phi)\right]^2$$

and

$$D(\Phi) = (1/\sqrt{2\pi T_d})d\, f_s(\Phi)/d\Phi = \exp\{\mathrm{irf}^2(2\Phi - 1)\}$$

Valid for $\Phi < \Phi_c = 1 - f_0$ (final explosive rupture regime)

$$f_a = \frac{f_0}{1-\Phi(t)} \qquad P_d(f) = \frac{1}{\sqrt{2\pi T_d}} \exp\left[-\frac{(1-f)^2}{2T_d}\right]$$

time to reach some Φ

$$\gamma T t = 4\pi\mu \int_0^{\Phi} D(z)U(z)\, e^{U(z)/T}\, dz$$

$$\gamma t \simeq 4\pi\mu \frac{D(\Phi)U(\Phi)}{A(\Phi)}\, e^{U(\Phi)/T}, \quad A(\Phi) = \frac{dU(\Phi)}{d\Phi}$$

for $\Phi < \Phi^*$ ← corresponds to minimum failure rate

This gives

$$U[\Phi(t)] = T \ln \gamma t \qquad (t < t^*)$$

γ obtained by matching with the initial state

$$\dot{\Phi} \simeq \frac{1}{4\pi\mu\, t\, \ln \gamma t} \exp\left[-\frac{1}{2T_d}\left(1 - f_0 - \sqrt{2T \ln \gamma t}\right)^2\right]$$

OMORI law: $1/t^p$ (apparent exponent <1)

From $\dot{\Phi} = R(\phi)$, minimum failure rate is solution of

$$dR(\Phi)/d\Phi = 0$$

$$D(\Phi^*)(1-\Phi^*)^2 = \alpha = \frac{f_0}{\sqrt{2\pi T_d}}$$

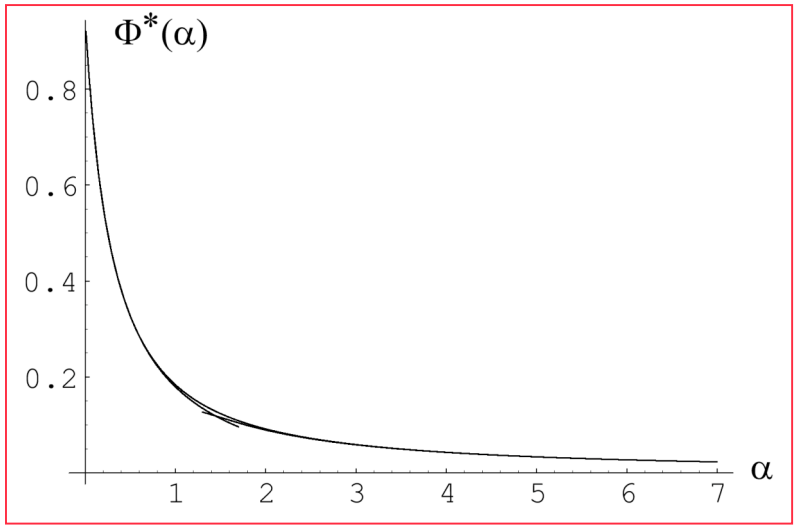

$$\Phi^*(\alpha) = \begin{cases} \dfrac{20-\pi-4(4-\pi)\alpha}{24-2\pi+8(4+\pi)\alpha}\,, & \alpha < 3/2\,, \\ \dfrac{1}{2}\,\mathrm{erfc}\left(\sqrt{\ln\alpha}\right)\dfrac{\alpha\sqrt{\pi\ln\alpha}}{1+\alpha\sqrt{\pi\ln\alpha}}\,, & \alpha > 3/2\,. \end{cases}$$

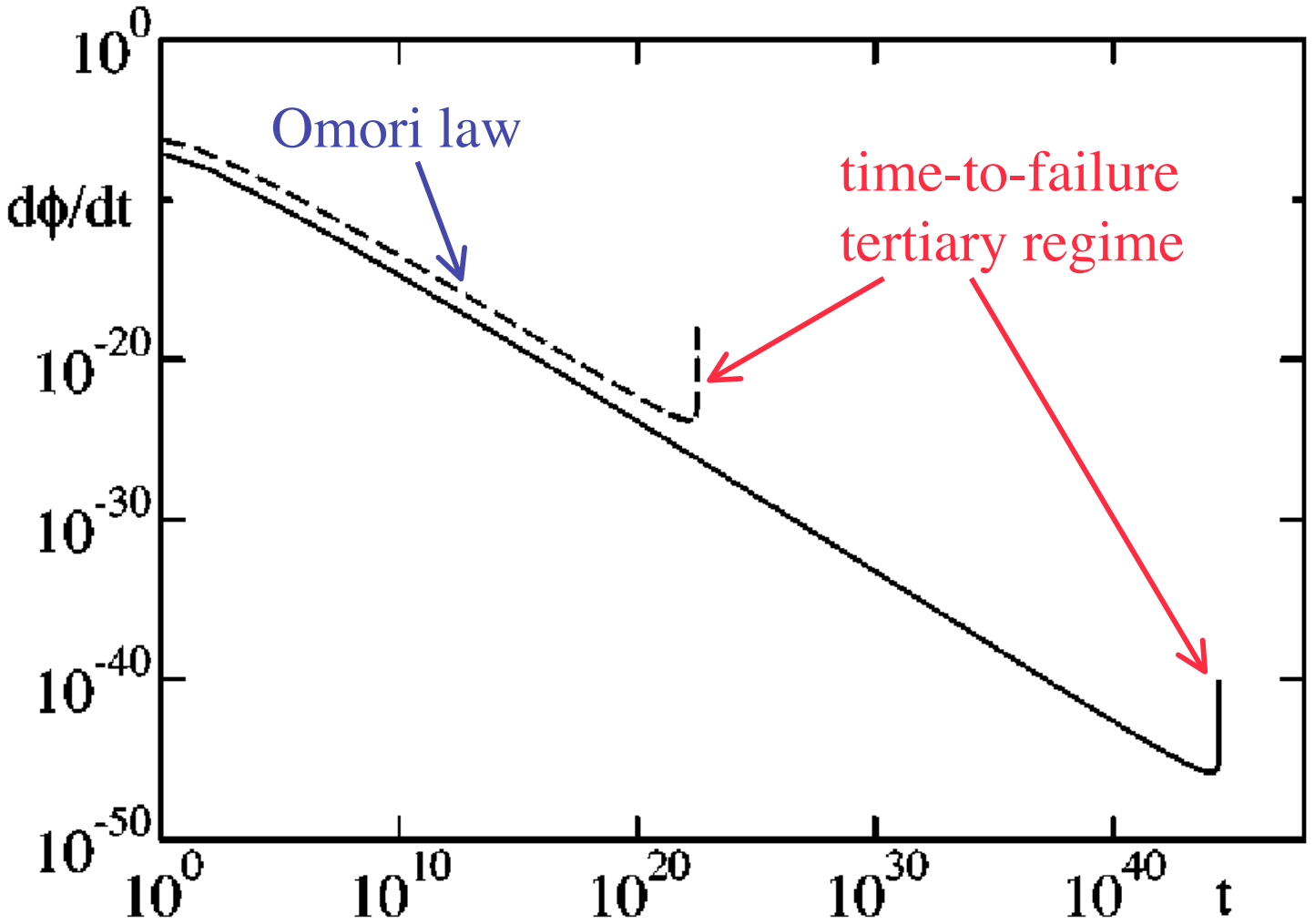

FIG. 2. Time derivative of Φ versus time for $T_d = 10^{-2}$ and two different values of the temperature, $T = 5 \times 10^{-4}$ (solid curve), $T = 10^{-3}$ (dashed curve).

POLITI, CILIBERTO, AND SCORRETTI
PHYSICAL REVIEW E **66**, 026107 (2002)

$$\gamma(t_c - t) = 4\pi\mu \int_{\Phi}^{\Phi_c} D(z)U(z)\, e^{U(z)/T}\, dz$$

$$\gamma(t_c - t) \simeq 4\pi\mu \frac{D(\Phi)U(\Phi)}{|A(\Phi)|}\, e^{U(\Phi)/T}, \qquad \Phi > \Phi^*$$

$$U\,[\Phi(t)] = T \ln[\gamma(t_c - t)] \qquad (\Phi^* < \Phi < \Phi_c)$$

$$\Phi_c - \Phi(t) = f_0 \frac{\sqrt{2T \ln \gamma(t_c - t)}}{1 - \sqrt{2T \ln \gamma(t_c - t)}}$$

$$\dot{\Phi}(t) = C(t)/(t_c - t)$$

$$C(t) = f_0\, T/[c(1-c)^2] \text{ with } c = \sqrt{2T \ln[\gamma(t_c - t)]}$$

Tertiary creep and finite-time to failure law

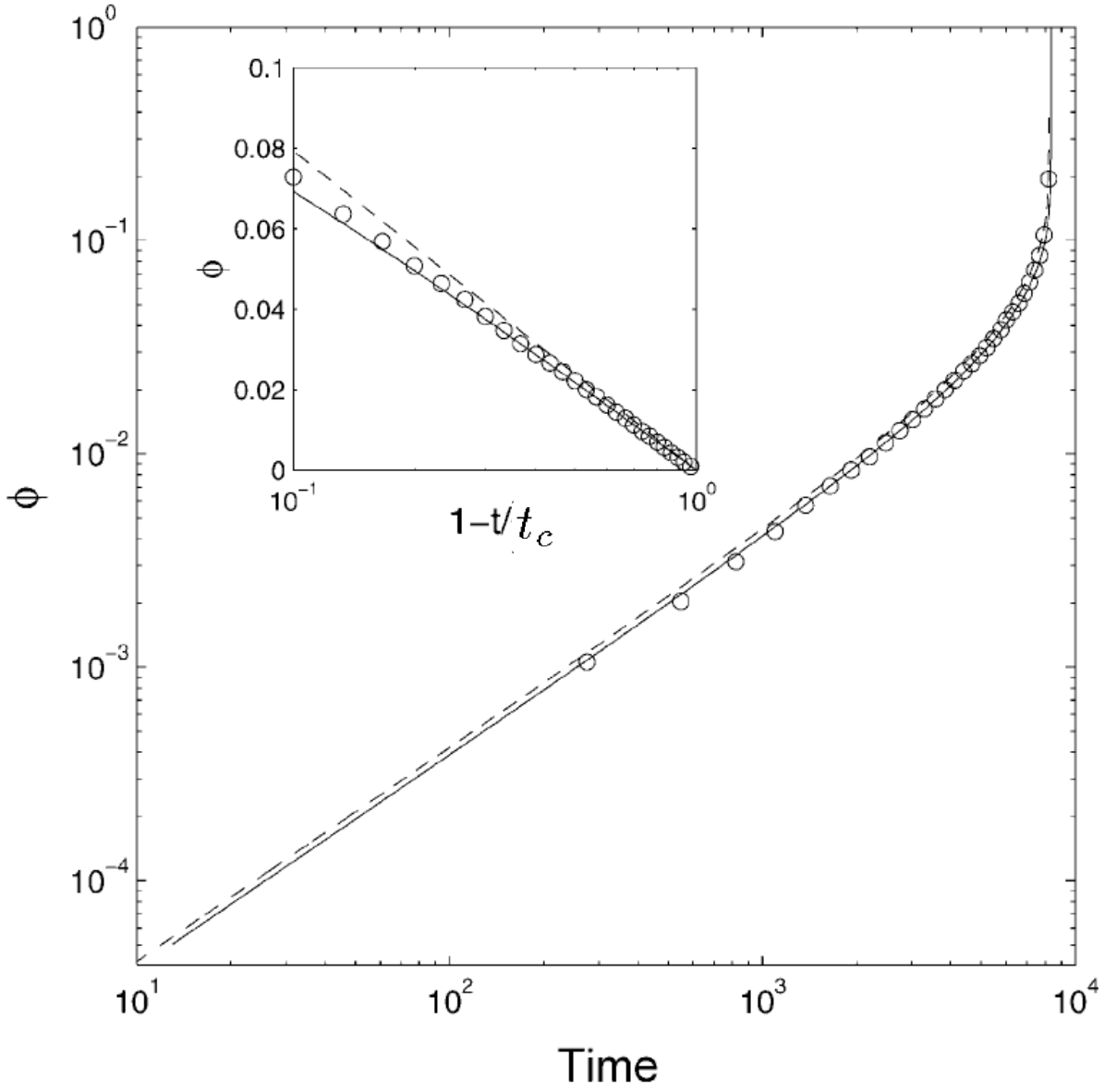

Fig. 3. Time evolution of ϕ at $f = 0.6$, $KT = 0.008$ and $KT_{\mathrm{d}} = 0$. The continuous line corresponds to a solution obtained by the numerical solution of Eq. (12). The dashed line is instead the approximated solution (Eq. (14)) of Eq. (12). The symbols (○) correspond to the results of the direct numerical simulation of the DFBM. These data are plotted in the inset as a function of $1 - t/\tau$ in a semi-log scale.

Dominant contribution to the total time to failure $\Phi \approx \Phi^*$

$$U(\Phi) = U(\Phi^*) - B(\Phi^*)(\Phi - \Phi^*)^2, \quad B(\Phi) = -\frac{1}{2}\frac{d^2U(\Phi)}{d\Phi^2}$$

$$\dot{\Phi} \simeq R(\Phi^*) \exp\left[-\frac{B(\Phi^*)}{T}(\Phi - \Phi^*)^2\right]$$

The solution of this equation is

$(\mathrm{erfi}\,(z) = \frac{1}{i}\,\mathrm{erf}\,(iz)$ is the imaginary error function)

$$\mathrm{erfi}\left(\sqrt{\frac{B(\Phi^*)}{T}}(\Phi - \Phi^*)\right) = 2\sqrt{\frac{B(\Phi^*)}{\pi T}}\,R(\Phi^*)\,(t - t^*)\,,$$

TOTAL LIFETIME: $$\gamma\, t_c = \frac{1}{R\,(\Phi^*)}\int_{-\infty}^{\infty} \exp\left[-\frac{B(\Phi^*)}{T}(\Phi - \Phi^*)^2\right] d\Phi$$

$$\gamma\, t_c \simeq 4\pi\sqrt{\pi}\,\frac{D(\Phi^*)U(\Phi^*)}{\sqrt{B(\Phi^*)}}\,\frac{\sqrt{T_d}}{T}\,\exp\left[-\frac{U(\Phi^*)}{T}\right]$$

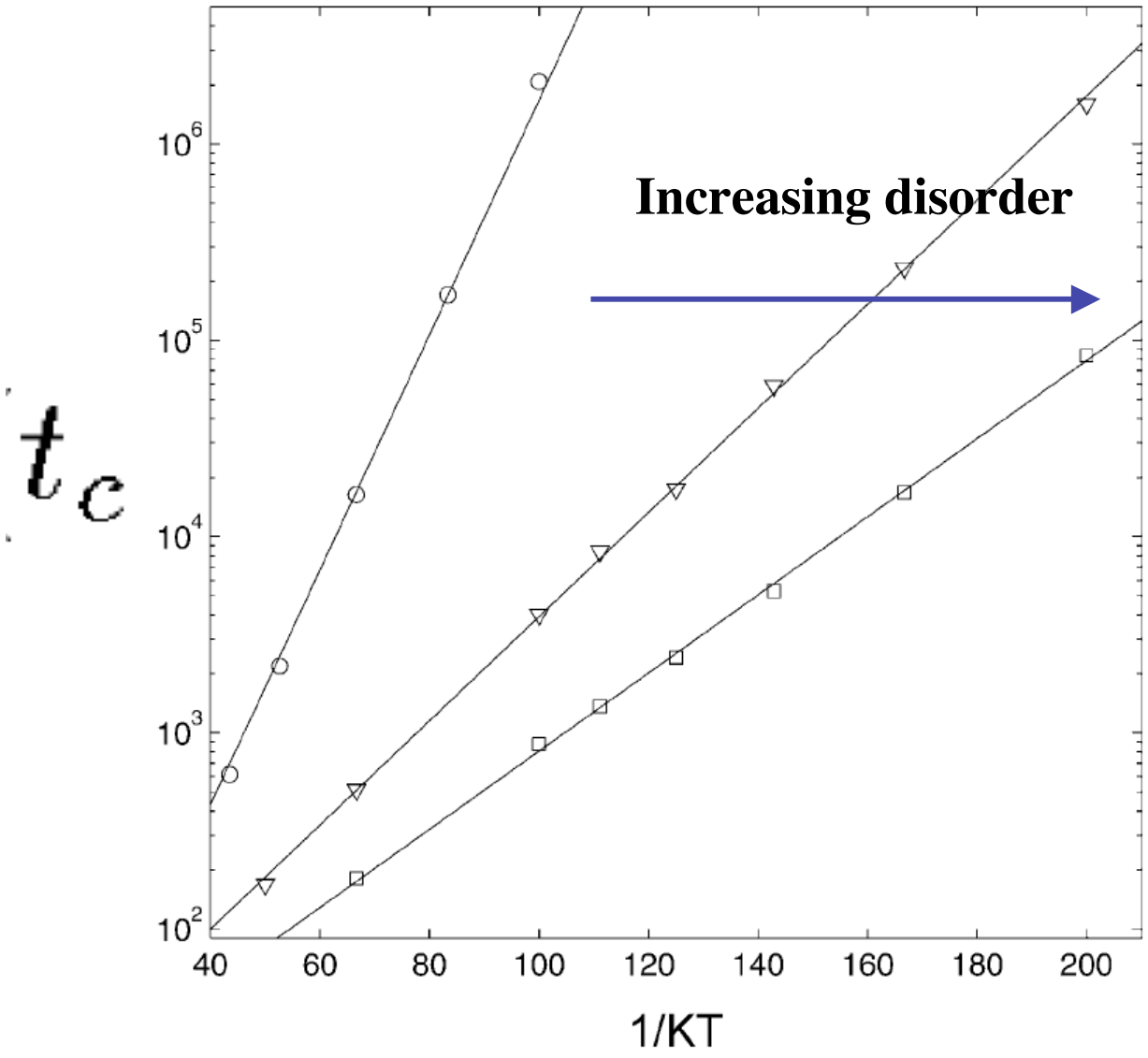

Fig. 4. Heterogeneous bundle ($KT_d \neq 0$). Dependence of the lifetime τ on $1/KT$ at $f_0 = 0.45$. The different symbols correspond to different values of KT_d: (○) $KT_d = 0$; (▽) $KT_d = 0.02$; (□) $KT_d = 0.04$. Notice that both τ and $d\tau/dKT$ decrease as KT_d increases, i.e., the more the media become heterogeneous, the smaller is τ and the dependence on KT of τ.

Thermal activation of rupture and slow crack growth in a model of homogeneous brittle materials

S. Santucci, L. Vanel, A. Guarino, R. Scorretti and S. Ciliberto

Europhys. Lett., **62** (3), pp. 320–326 (2003)

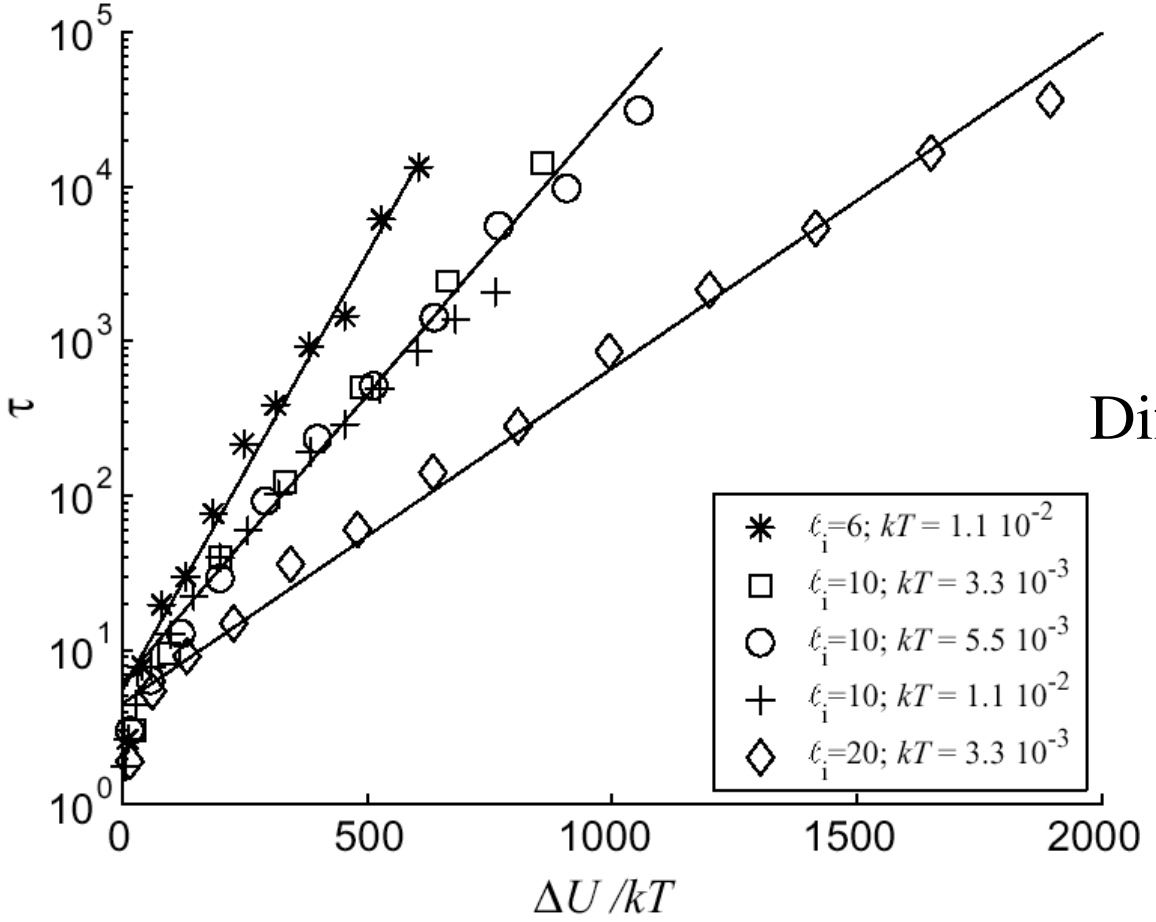

Different crack lengths

Fig. 1 – Logarithm of lifetime as a function of the energy barrier as predicted by eq. (2). Failure of data to scale with initial crack length is the main observation. Straight lines are a guide for the eye.

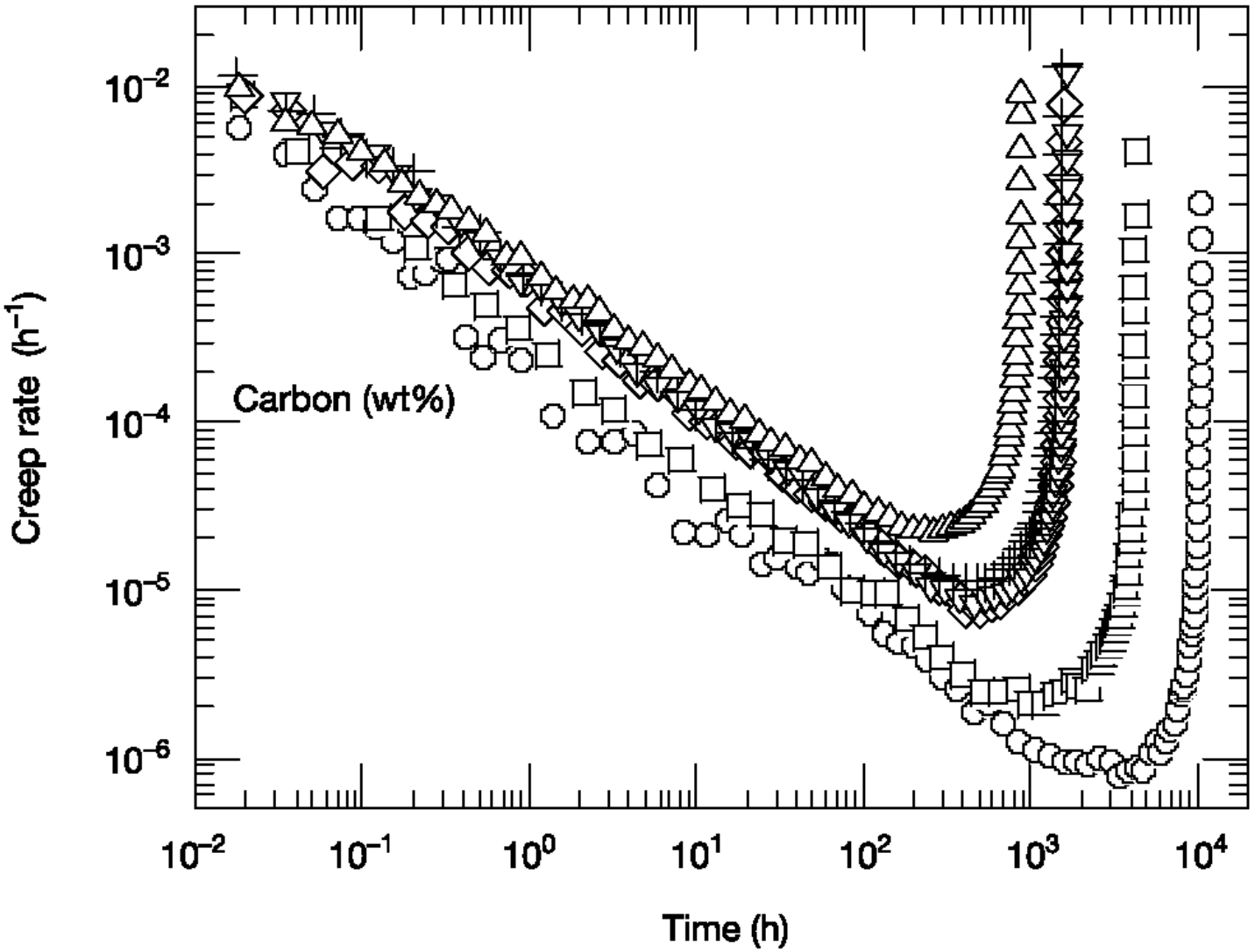

Figure 1 Creep rate versus time curves of at 923 K and 140 MPa. Circles, 0.002% C; squares, 0.018% C; diamonds, 0.047% C; inverse triangles, 0.078% C; crosses, 0.120% C; triangles, 0.160% C. The base composition of the steels was Fe–9% Cr–3% W–3% Co–0.2% V–0.06% Nb–0.05% N.

Taneike et al. Nature (2003)

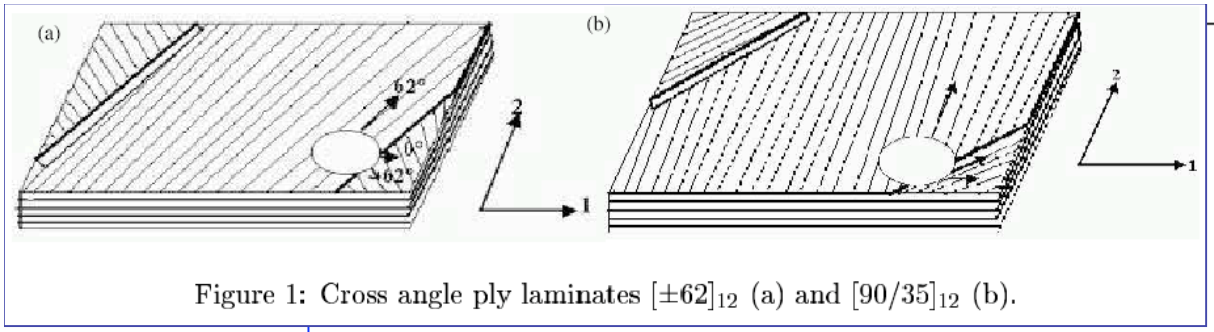

Figure 1: Cross angle ply laminates $[\pm 62]_{12}$ (a) and $[90/35]_{12}$ (b).

Figure 4: Creep strain and AE response for [90/35] angle ply composite #3. The thin solid line is the deformation (left axis), the heavy black line is the cumulated AE count (right axis) and dashed line is the cumulated energy (arbitrary units).

H. Nechad, A. Helmstetter, R. El Guerjouma and D. Sornette (2004)

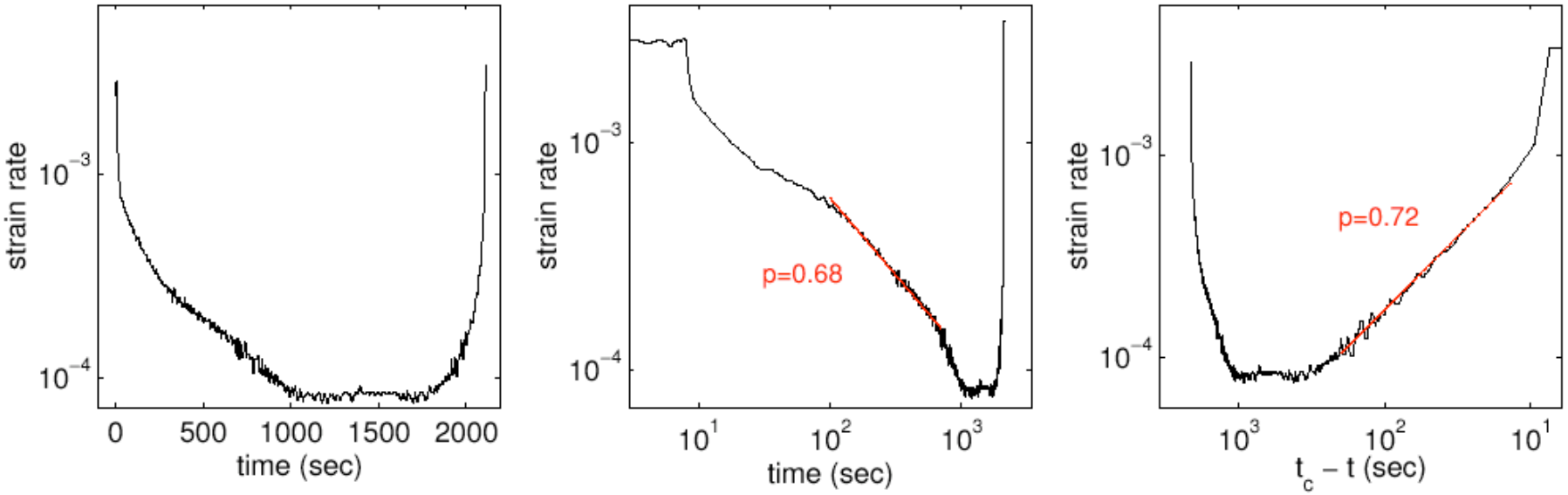

Figure 6: Creep strain rate for [90/35] angle ply composite #3

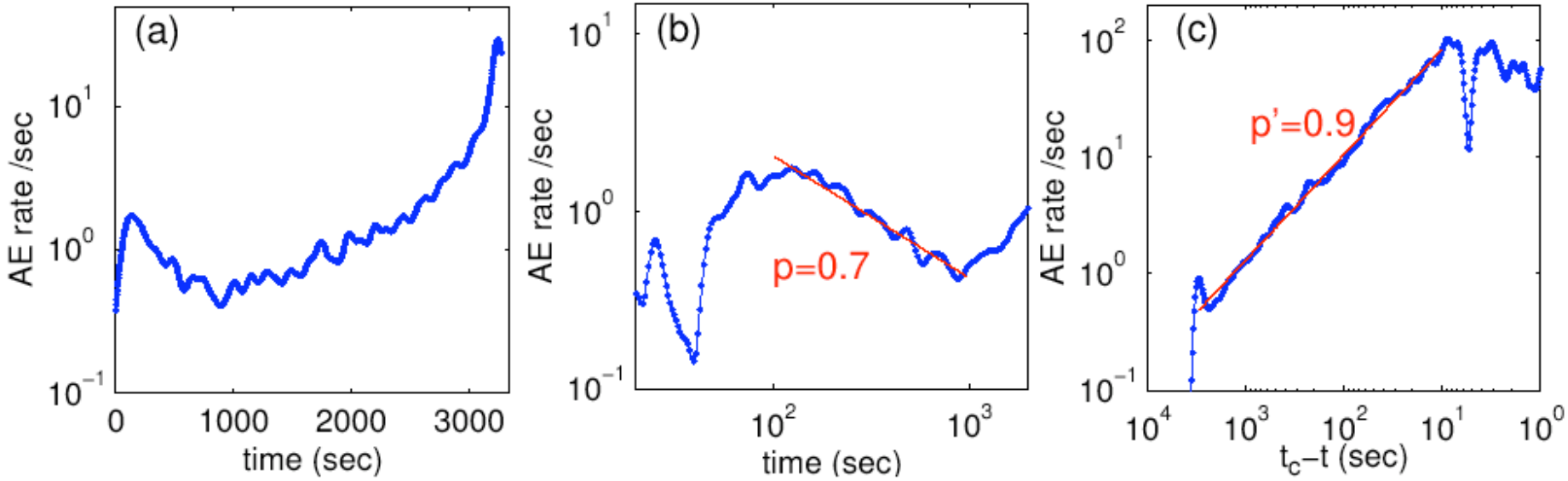

Figure 8: Rate of AE events for [90/35] angle ply composite #3. We use different axes to illustrate Andrade law in the primary creep regime $dN/dt \sim 1/t^p$ (b) and the power-law singularity of the AE rate before failure $dN/dt \sim 1/(t_c - t)^{p'}$. H. Nechad, A. Helmstetter, R. El Guerjouma and D. Sornette (2004)

Eyring rheology

$$\frac{\mathrm{d}e}{\mathrm{d}t} = K \sinh\left(\frac{\beta s}{e_{01}^{\mu}}(e + e_{02})^{\mu} - \beta E e\right)$$

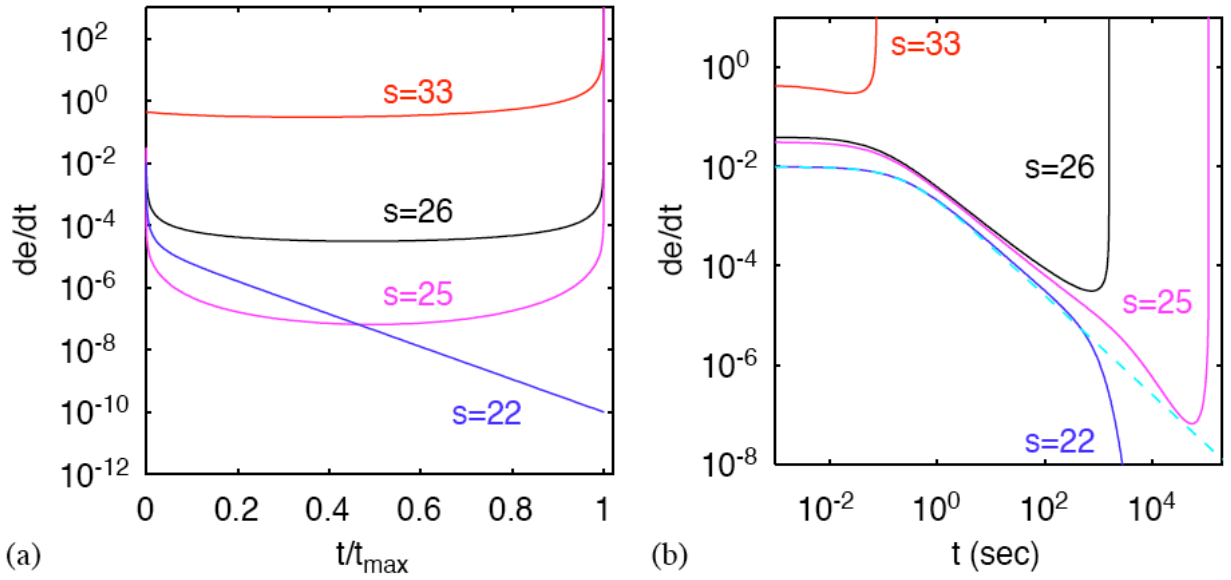

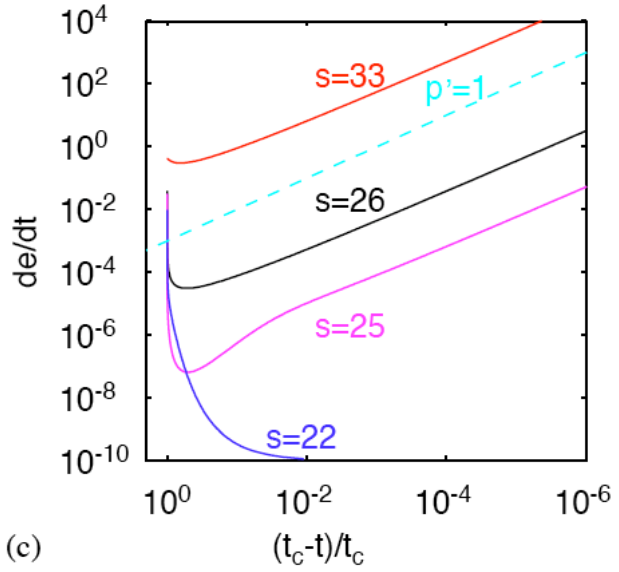

H. Nechad, A. Helmstetter, R. El Guerjouma and D. Sornette
Andrade and Critical Time-to-Failure Laws in Fiber-Matrix Composites: Experiments and Model,
Journal of Mechanics and Physics of Solids (JMPS) 53, 1099-1127 (2005)

H. Nechad, A. Helmstetter, R. El Guerjouma and D. Sornette (2004)

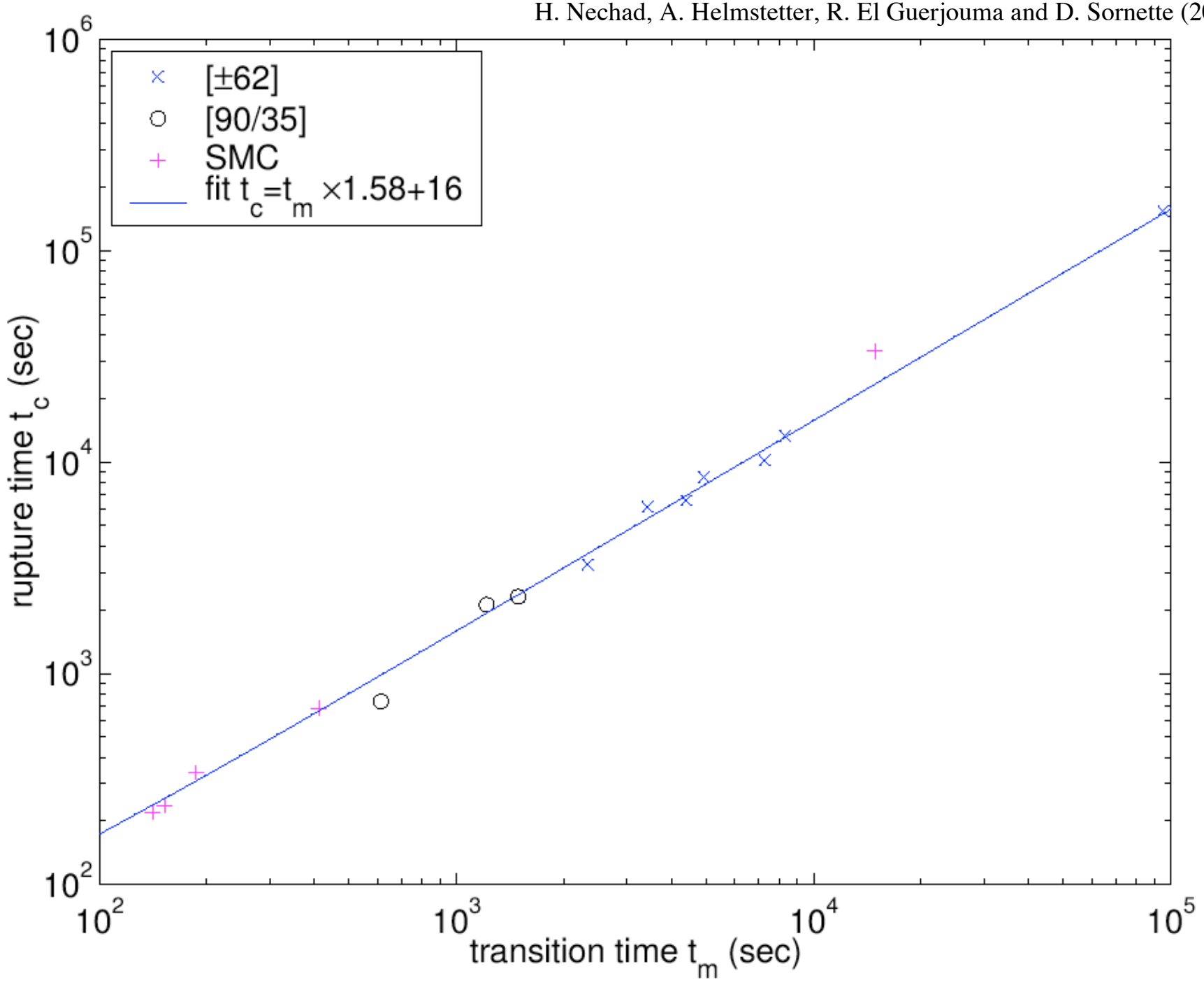

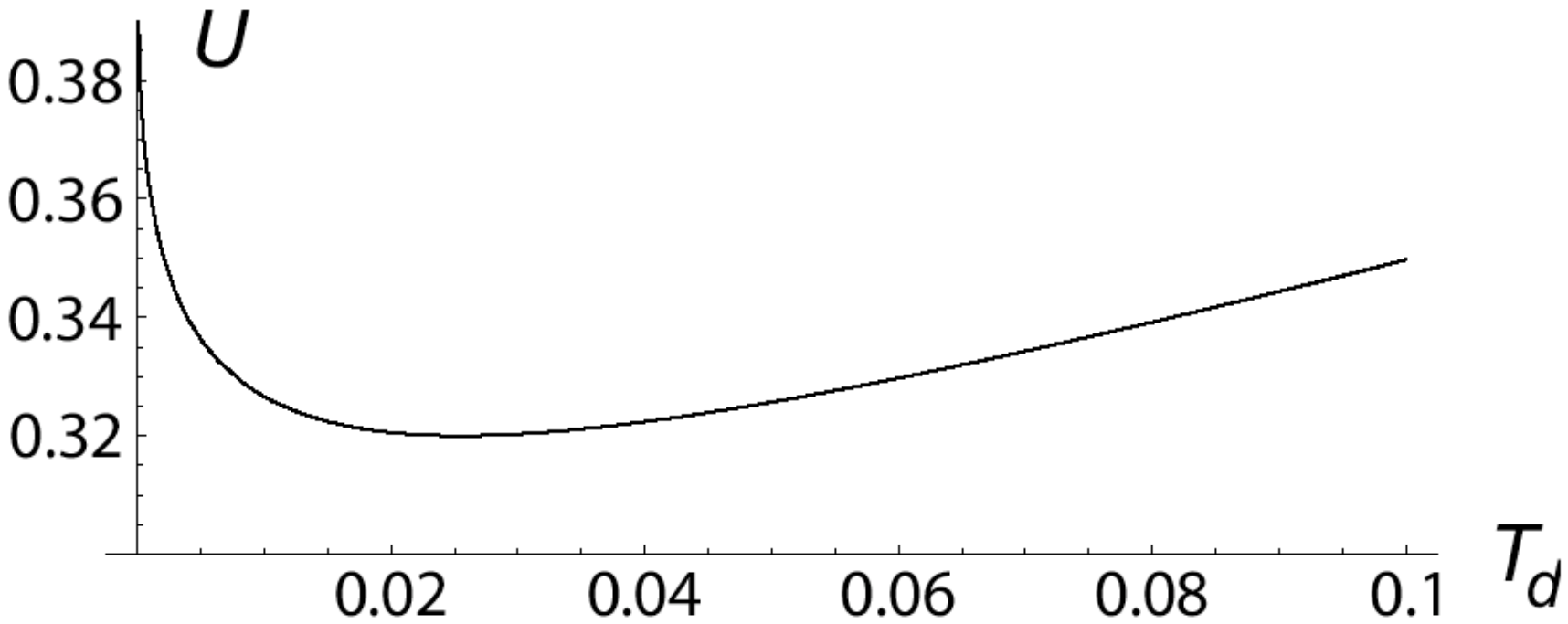

FIG. 1: Effective barrier energy $U(\Phi^*)$ as a function of the disorder strength T_d, in the case where $\Phi^* = 1/2$, corresponding to $T_d^* = \frac{8}{\pi} f_0^2$, for $f_0 = 0.1$ leading to $T_d^* \simeq 0.025$. This illustrates the non-monotonous behavior of $U(\Phi^*)$ and thus of the lifetime t_c with T_d.

Frozen disorder enhances/renormalizes thermal fluctuations but also act as rupture barriers

Summary

- Quenched disorder T_d is a relevant parameter!
- Annealed disorder T is a relevant parameter
- Renormalization/amplification of T by T_d
- Theory of both primary and tertiary regime
  - Primary: controlled by the thermally activated stress transfer on the weakest elements
  - Tertiary: controlled by the cascade of failures
- Consequences of longevity/prediction

Spatial and temporal organization of seismicity in Californie

Landers
28 june 1992
M=7.3

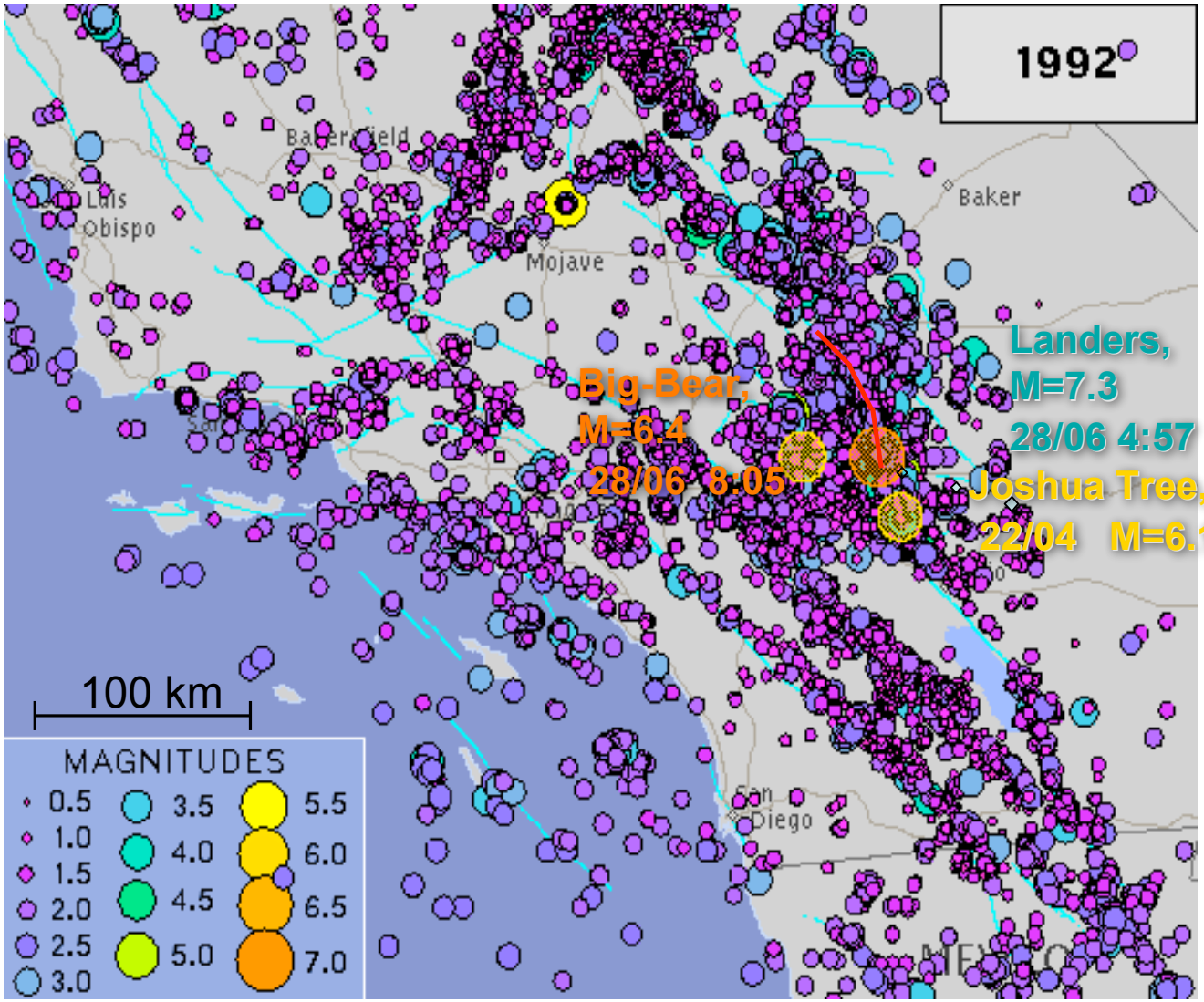

Seismicity rate per day in Southern California M>2

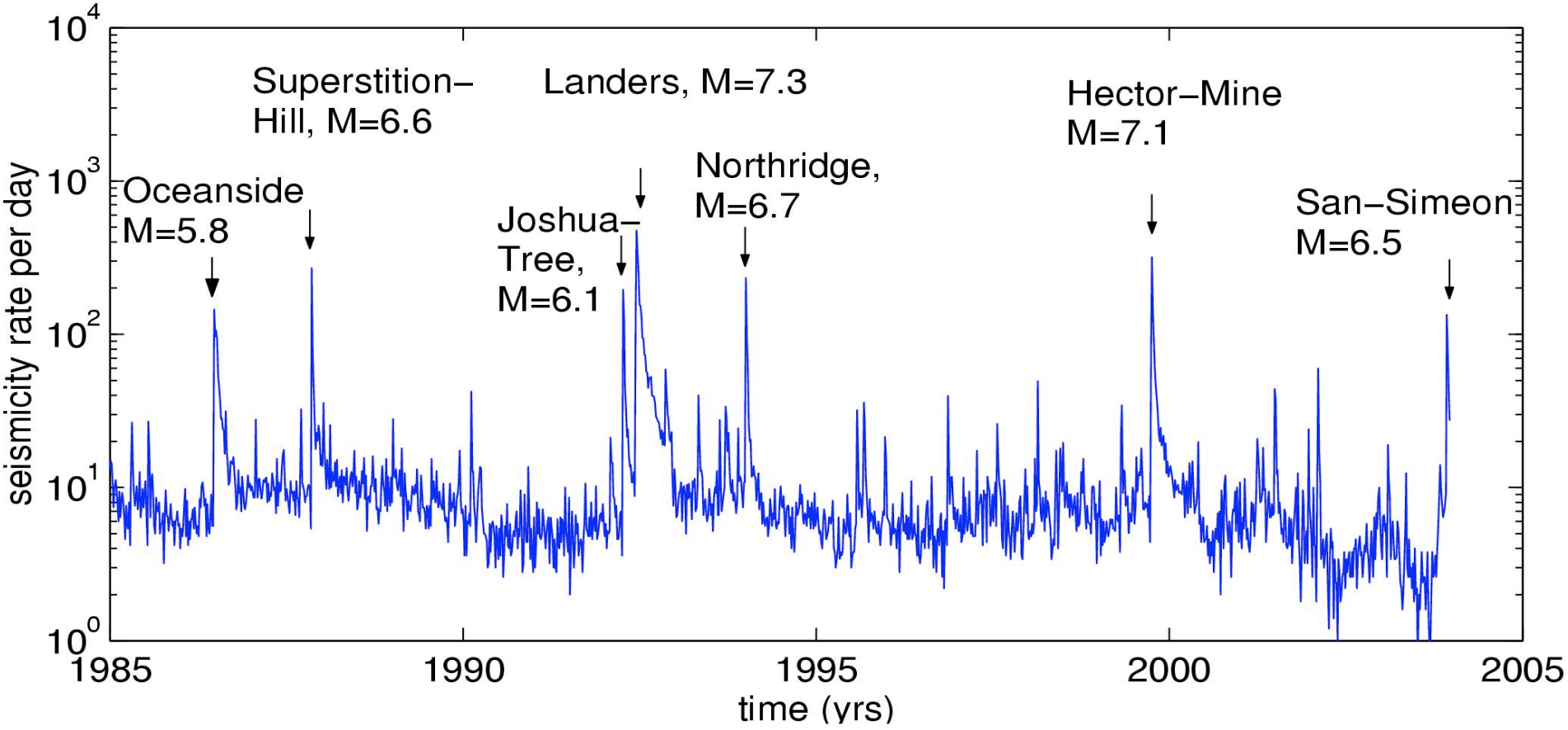

The Physics of Stress-Aided Thermal Activation of Rupture

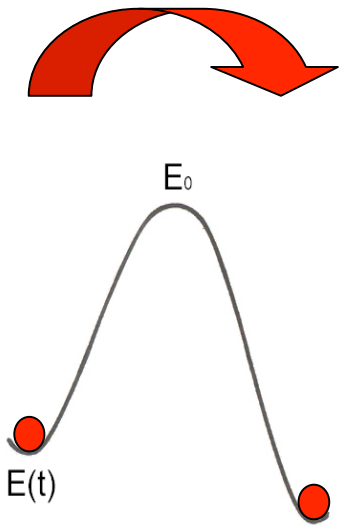

In order to reach a state of lower energy, some microscopic physical systems must overcome an energy barrier.

The rate at which this is done depends **exponentially on the height of the barrier**, as well as on **the inverse of temperature**.

$$\lambda(t) = \lambda_0 \exp\left(-\frac{E_0 - E(t)}{kT}\right)$$

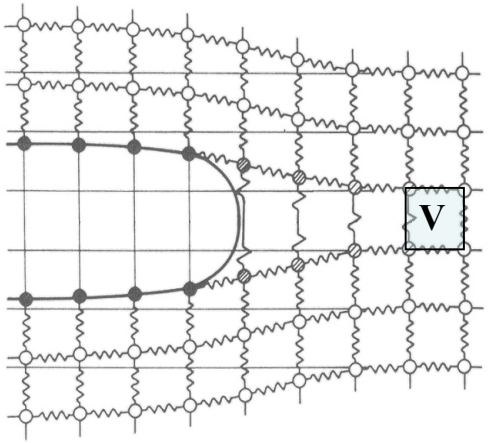

For example, the rate at which a bond breaks at a crack tip depends on the driving stress applied on that bond, its strength and temperature.

We simply assume that the relationship between the seismicity rate and the applied stress follows the same kind of law.

$$\lambda(t) = \lambda_0 \exp\left(-\frac{\sigma_0 - \sigma(t)}{kT} V\right)$$

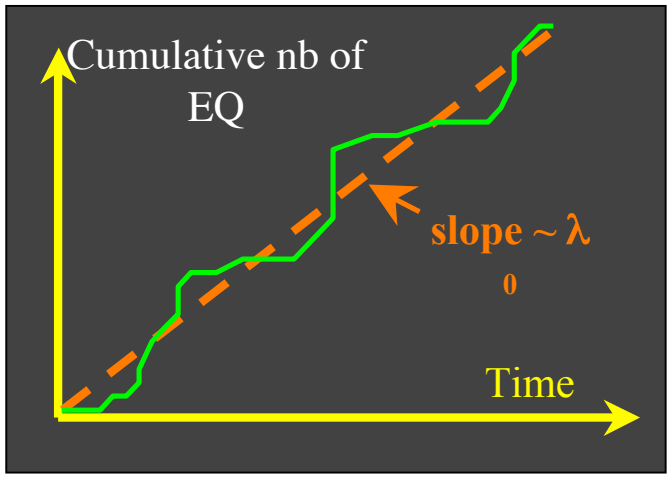

λ_0 ~ mean seismicity rate - $\lambda(t)$: seismicity rate - σ_0 : strength

$\sigma(t)$: applied stress - V : activation volume - T : temperature

Thermally activated multifractal rupture process

G. Ouillon and D. Sornette, Magnitude-Dependent Omori Law: Theory and Empirical Study, J. Geophys. Res., 110, B04306, doi:10.1029/2004JB003311 (2005); Multifractal Scaling of Thermally-Activated Rupture Processes, Phys. Rev. Lett. 94, 038501 (2005)

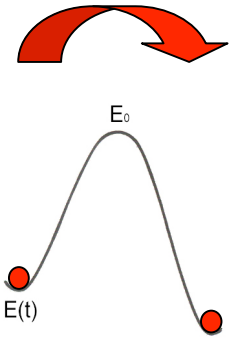

Intensity (average conditional seismicity rate)

At position r and time t

$$\lambda(\vec{r},t) \sim \exp\left[-\beta E(\vec{r},t)\right]$$

$$E(\vec{r},t) = E_0(\vec{r}) - V\Sigma(\vec{r},t) \quad \text{(Zhurkov, 1965)}$$

(due to stress corrosion, damage, state-and-velocity dependent friction and mechano-chemical effects

$$\Sigma(\vec{r},t) = \Sigma_{\text{far field}}(\vec{r},t) + \int_{-\infty}^{t}\int dN[d\vec{r}\,' \times d\tau]\Delta\sigma(\vec{r}\,',\tau)g(\vec{r}-\vec{r}\,',t-\tau)$$

$$g(\vec{r},t) = f(\vec{r}) \times h(t)$$

And sum over all spatial positions of sources gives

$$\lambda_i(t) = \lambda_{\text{tec}}(t)\exp\left[\beta\sum_j\int_{-\infty}^{t} d\tau\ \Delta\sigma_j(\tau)\ g_{ij}(t-\tau)\right]$$

Generalization of stress release models [Vere-Jones et al.]

Our Physical Picture of Seismicity

- The **rupture** of each event **is thermally activated**, driven by stress.
- Each shock induces instantaneously a **burst of aftershocks,** which amounts to 10^{qM} events.
- At each location, **stress fluctuations** due to previous events are distributed as:

$$P(\sigma)\,d\sigma \approx \frac{C}{(\sigma+\sigma_0)^{1+\mu}}\,d\sigma$$

- The **rheology is viscoplastic**, with a relaxation function featuring a very large relaxation time τ_M :

$$h(t) = \frac{h_0}{(t+t_1)^{1+\theta}} \exp\left(-\frac{t}{\tau_M}\right) \qquad \theta = -1/2 + \varphi$$

- At any place *r* and any time *t*, **the seismicity rate** (on the left-hand side) **depends exponentially on the stress fluctuations** due to past earthquakes, mediated by the relaxation function:

This picture takes account of the fact that earthquakes generate stress fluctuations, which in turn modify the stress state in a feedback loop and cascading process, involving the whole history of the system.

$$\lambda(r,t) = \lambda_{tec} \exp\left[\frac{V}{kT}\sum_{passé}\sigma(t_i)h(t-t_i)\right]$$

Theoretical predictions using tail covariance (Ide-Sornette, 2001)

$$\Pr[\lambda(t) > \lambda_q | \lambda_M] = \Pr[e^{\beta\omega(t)} > \frac{\lambda_q}{\lambda_{\rm tec}} | \omega_M] = \Pr[\omega(t) > (1/\beta) \ln \left(\frac{\lambda_q}{\lambda_{\rm tec}} \right) | \omega_M]$$

$$\lambda_q(t) = A_q \ \lambda_{\rm tec} \ e^{\beta\gamma(t)\omega_M}$$

$$\gamma(t) = \frac{h_0^2}{\Delta t^{2/\mu}} \left(\frac{1}{t^{2m-1}} \int_{c/t}^{\frac{T+c}{t}-1} dy \frac{1}{(y+1)^m} \frac{1}{y^m} \right)^{\frac{2}{\mu}}$$

$$m = (1+\theta)\mu/2.$$

Since $\gamma(t) \sim \ln(t)$ and $\omega_m \sim M$, we obtain $p(M) = a M + b$

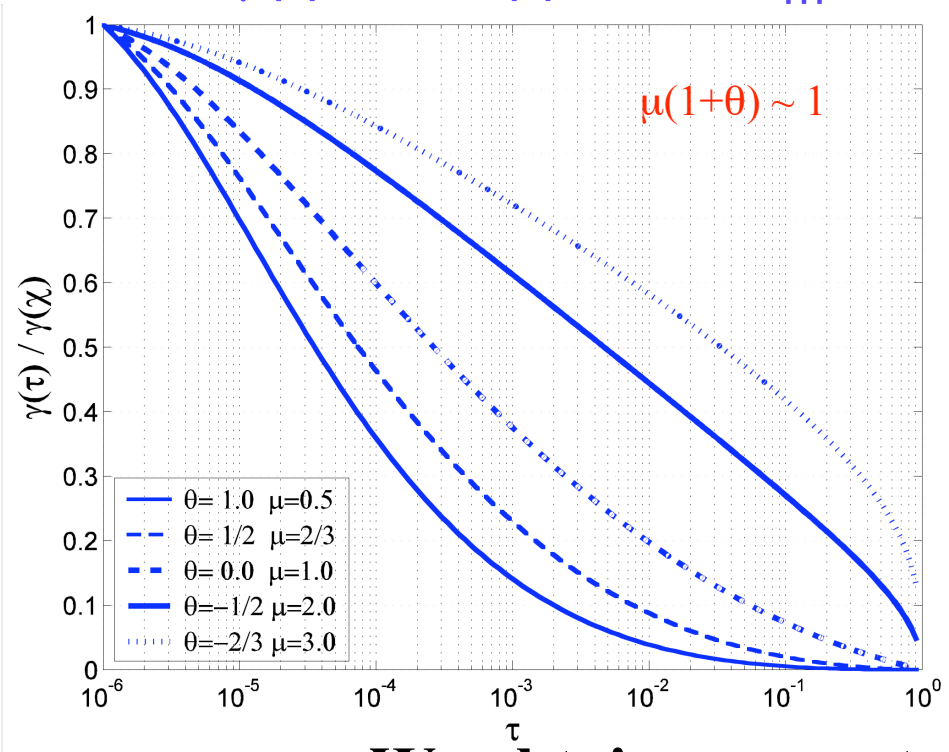

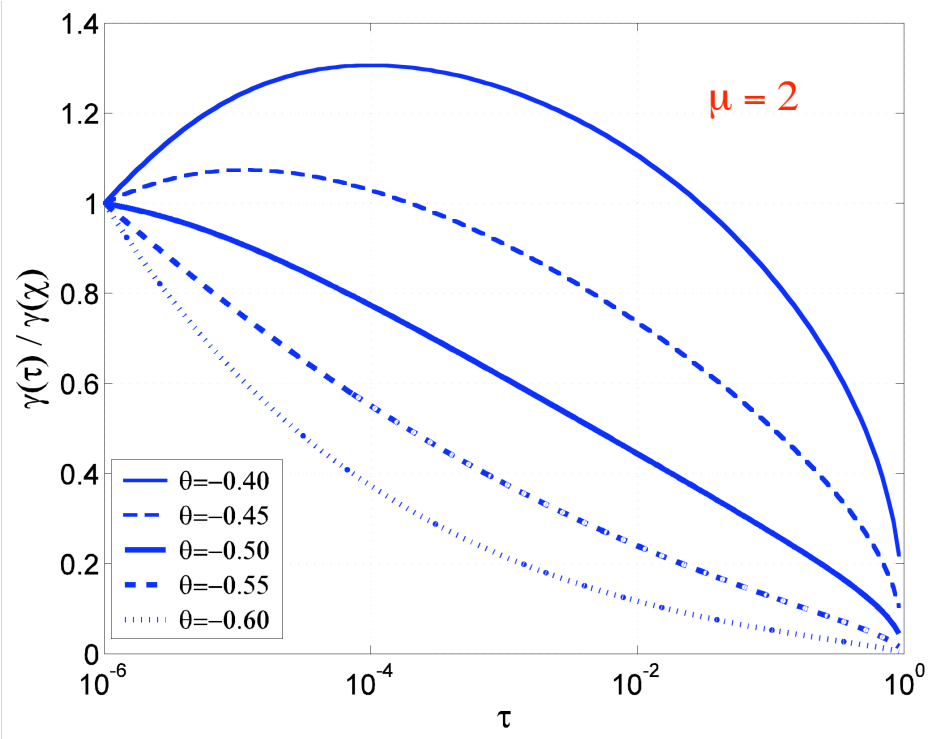

We obtain an exact multifractality if $\mu(1+\theta) \sim 1$

Stacked Triggered Seismicity Sequences

Large events trigger enough aftershocks to allow us to compute a *p* exponent – but this is not the case for low-magnitude main events.

So we prefer to follow a **stacking strategy to improve the signal to noise ratio** :

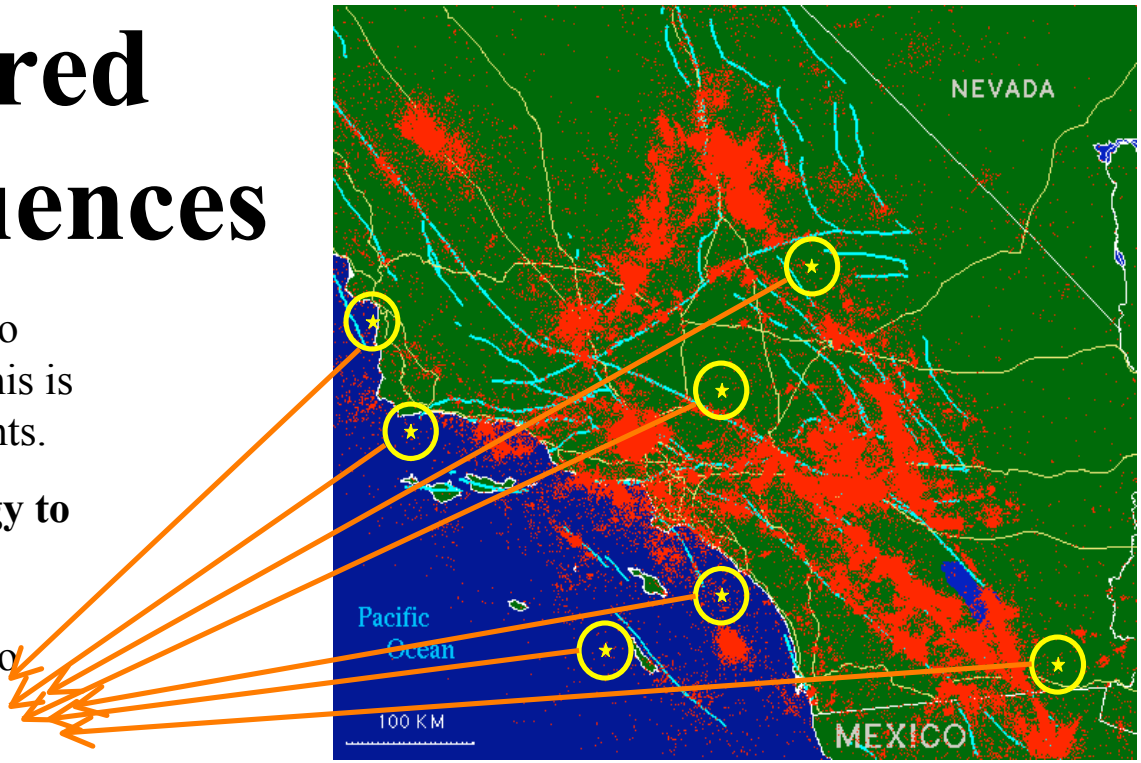

• look for isolated mainshocks according to magnitude range

• select and stack aftershocks sequences

• fit the stacks with :

$$N(t) = A\, t^{-p} + B$$

where B accounts for a constant background noise

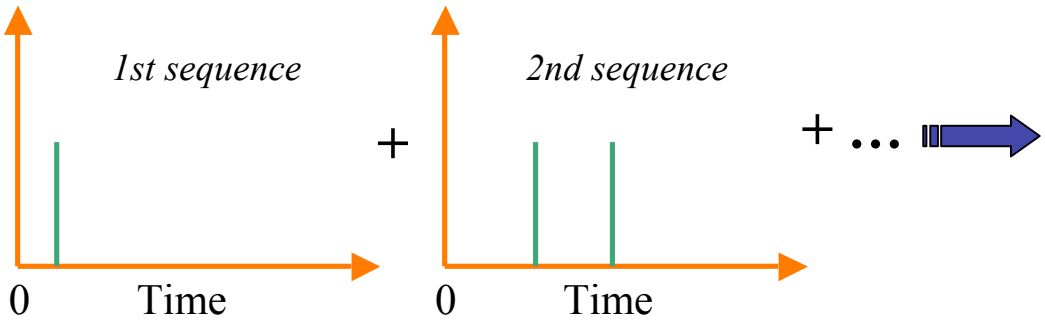

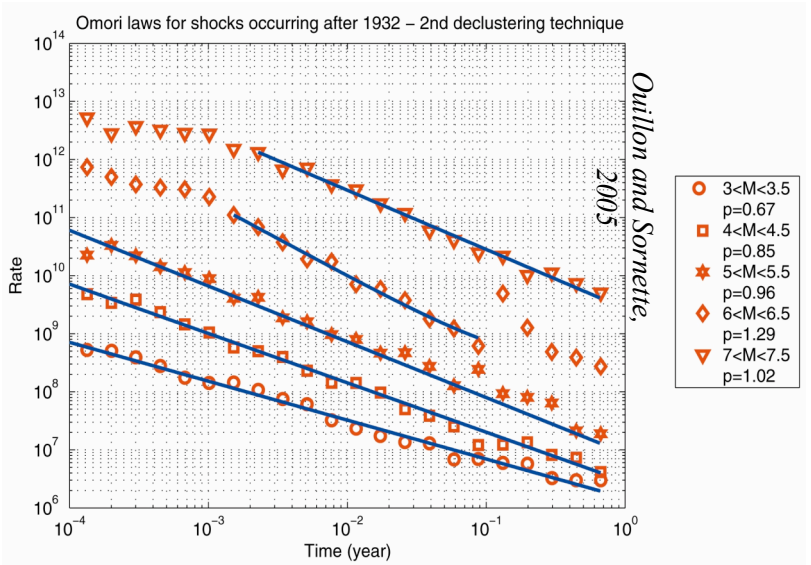

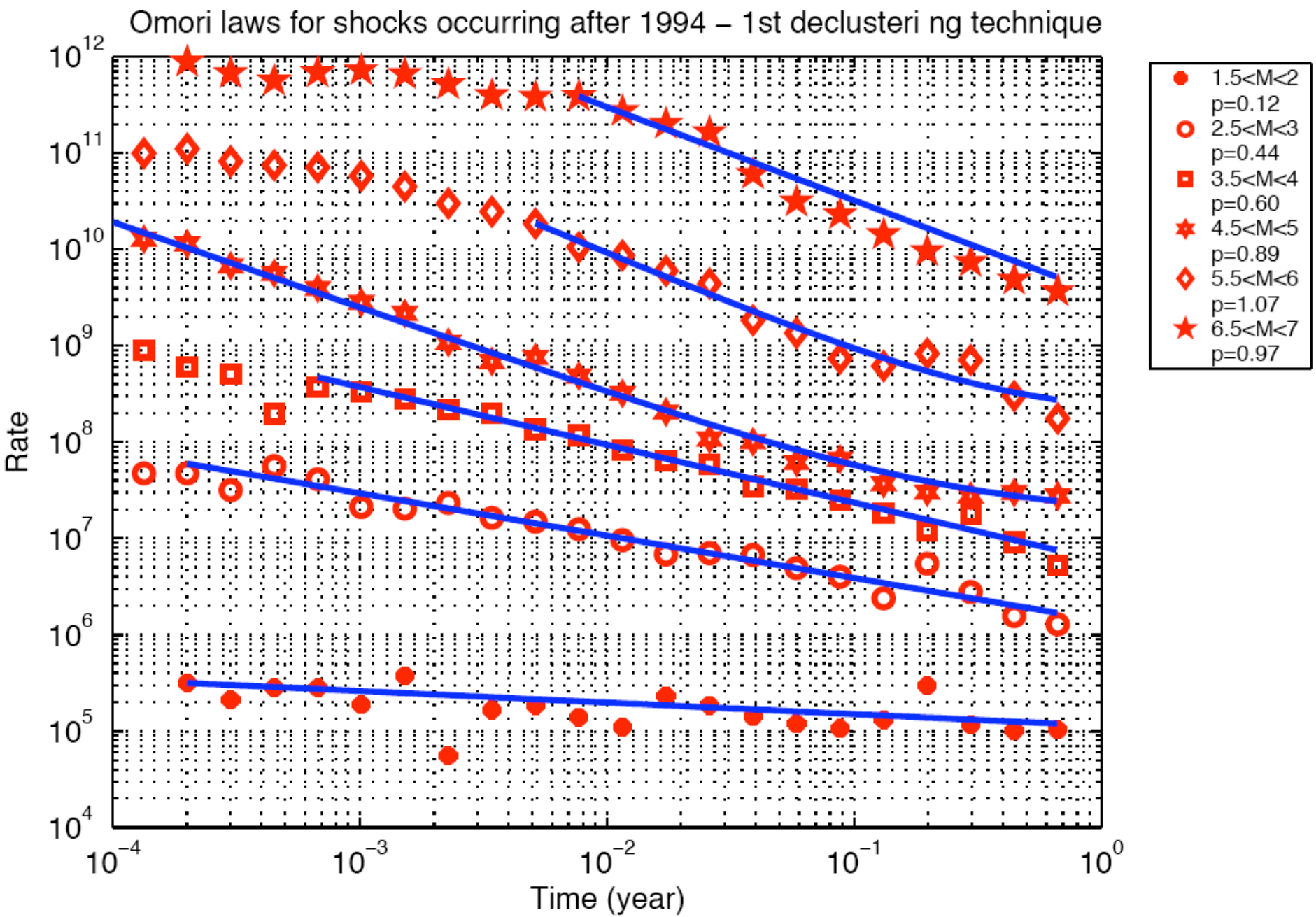

D. Sornette and G. Ouillon, Multifractal Scaling of Thermally-Activated Rupture Processes, Phys. Rev. Lett. 94, 038501 (2005)

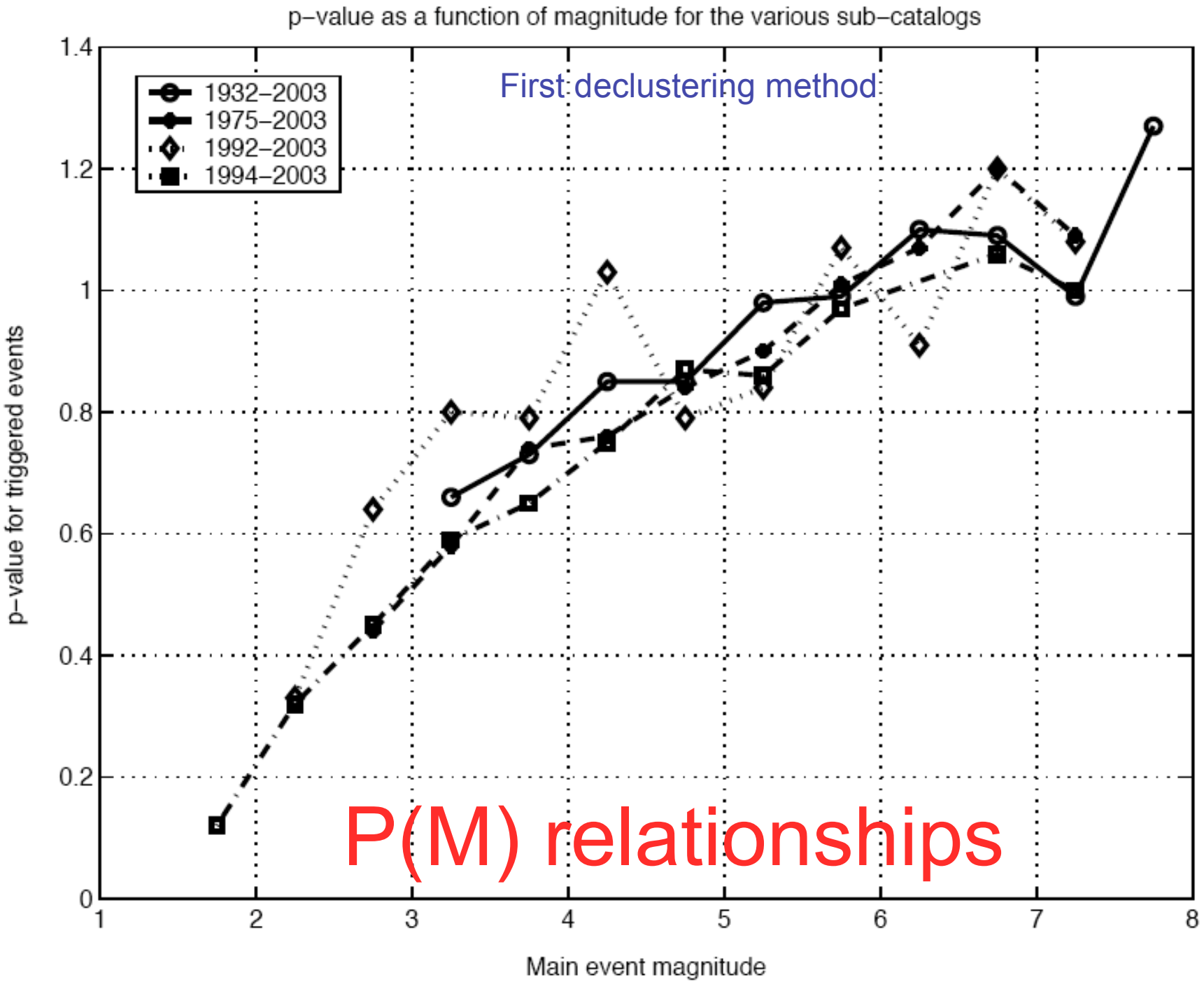
p−value as a function of magnitude for the various sub−catalogs
First declustering method
1932−2003
1975−2003
1992−2003
1994−2003
p−value for triggered events
Main event magnitude
0
0.2
0.4
0.6
0.8
1
1.2
1.4
1
2
3
4
5
6
7
8
P(M) relationships

p(M) = aM + b

We processed three catalogs, that we pre-processed to check for their completude and its evolution with time.
We then computed stacked aftershocks time series, sorting them within intervals of 0.5 magnitude amplitudes.

We clearly observed a linear dependence of *p* with magnitude M.

Statistical tests have been performed using a bootstrap strategy, and we were able to show that all slopes were significantly different from 0, and that all linear relationships were significantly different from each other.

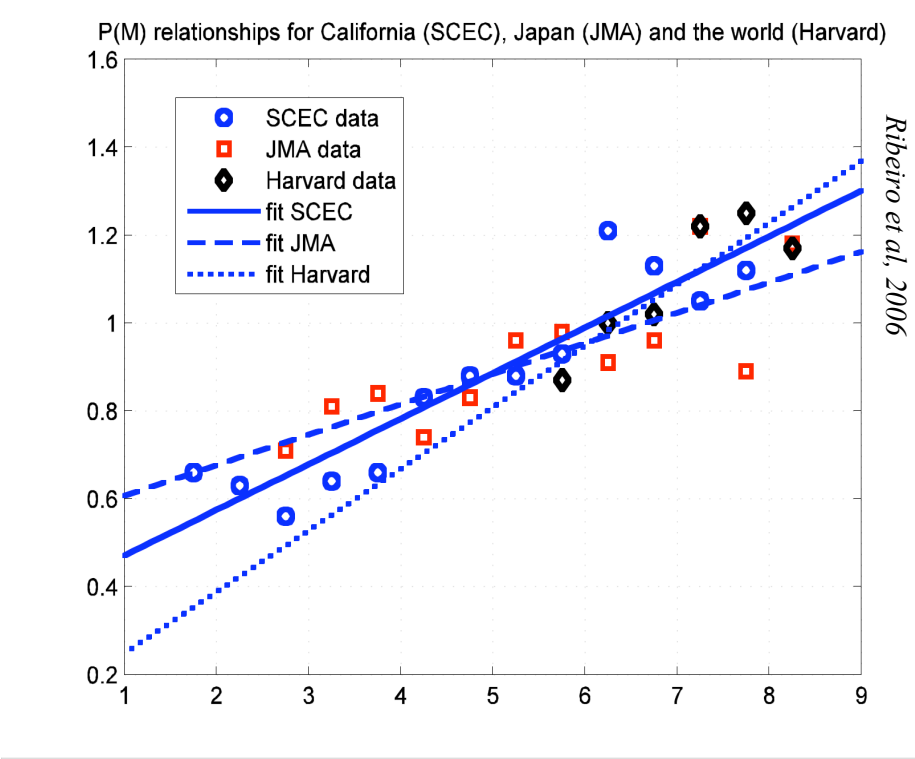

For Southern California (SCEC catalog):

p(M) = 0.10M + 0.37

For Japan (JMA catalog):

p(M) = 0.07M + 0.54

For the World (Harvard catalog):

p(M) = 0.14M + 0.11

μ(1+θ) : evidence of self-organization ?

$$P(\sigma)\,d\sigma \approx \frac{C}{(\sigma+\sigma_0)^{1+\mu}}\,d\sigma$$

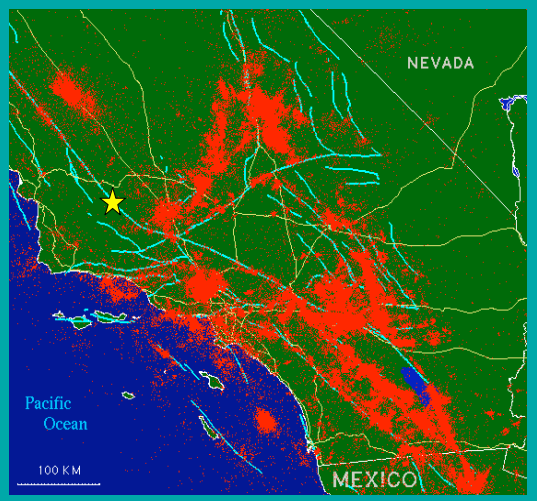

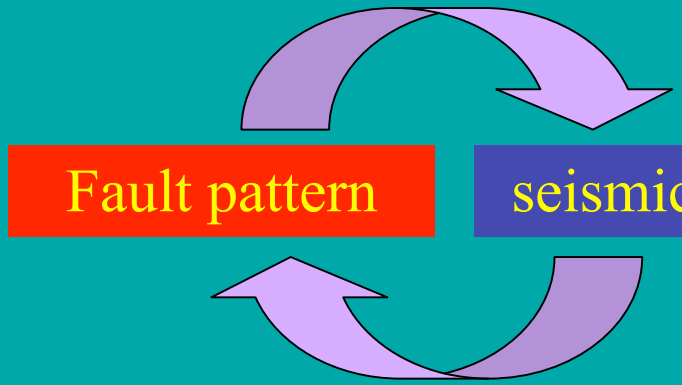

$$h(t) = \frac{h_0}{(t+t_1)^{1+\theta}} \exp\left(-\frac{t}{\tau_M}\right)$$

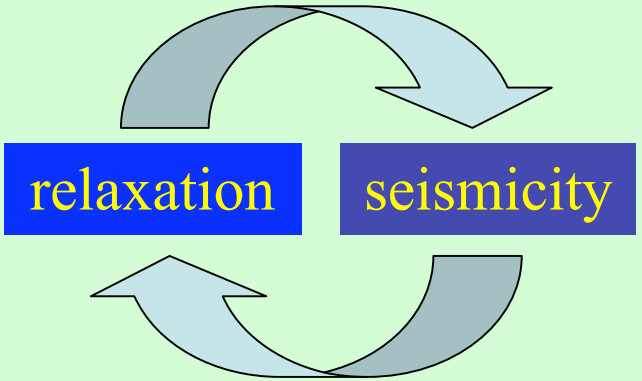

μ controls stress fluctuations, which mainly depend on the spatial structure of the fault network over which events occur – which make the fault pattern grow (left).

θ controls the stress relaxation in rocks. Stress determines the seismicity rate, but earthquakes are themselves part of the stress relaxation complex process (top).

All in all, the condition μ(1+θ) ~ 1 reflects the critical self-organization of brittle processes in the earth's crust.

Conclusions

- The multifractal time distribution of earthquakes implies that **the exponent *p* of the Omori law increases with the magnitude M of the mainshock.**
- Empirical data observations on various catalogs suggest that *p* linearly increases with M: **$p(M) = aM + b$**
- We proposed a physical model where the **seismicity rate depends exponentially on stress and on inverse temperature**, and where **the rheology is viscoplastic** with a slow relaxation.
- A condition **linking the fault network geometry and the rheology of the tectonic system** emerges to explain such a multifractal phenomenology : **$\mu(1+\theta) \sim 1$** – we speculate that it is a **fundamental equation of self-organized criticality.**
- For the first time, a physical microscopic model is proposed that is able to explain earthquakes time dynamics at all scales.

References:

G. Ouillon and D. Sornette: Magnitude-dependent Omori law: Theory and empirical study, J. Geophys. Res., VOL. 110, B04306, doi:10.1029/2004JB003311, 2005

E. Ribeiro, G. Ouillon and D. Sornette: New empirical results on the magnitude-dependent Omori law, submitted to Geophys. Res. Lett.,

A.S. Krausz and K. Krausz: Fracture kinetics of crack growth, Kluwer, 1987

Stein, R. S.: Earthquake conversations, Sci. Am., 288(1), 72–79, 2003